

Journal of Visualized Experiments

2-photon imaging of microglial processes attraction toward ATP or serotonin in acute brain slices --Manuscript Draft--

Article Type:	Invited Methods Article - JoVE Produced Video
Manuscript Number:	JoVE58788R1
Full Title:	2-photon imaging of microglial processes attraction toward ATP or serotonin in acute brain slices
Keywords:	microglia; multiphoton microscopy; acute brain slices; chemoattraction; motility; morphology; serotonin; ATP; live imaging; time-lapse imaging.
Corresponding Author:	Anne Roumier Institut du Fer a Moulin Paris, FRANCE
Corresponding Author's Institution:	Institut du Fer a Moulin
Corresponding Author E-Mail:	anne.roumier@inserm.fr
Order of Authors:	Fanny Etienne Vincenzo Mastrolia Luc Maroteaux Jean-Antoine Girault Nicolas Gervasi Anne Roumier
Additional Information:	
Question	Response
Please indicate whether this article will be Standard Access or Open Access.	Standard Access (US\$2,400)
Please indicate the city, state/province, and country where this article will be filmed . Please do not use abbreviations.	Paris, France

Dr Anne Roumier
Institut du Fer à Moulin
17 rue du Fer à Moulin
75005 Paris, France
+ 33 1 45 87 61 24
+33 6 15 10 33 98
Anne.roumier@inserm.fr



Dear editors,

It's my pleasure to resubmit to JoVE the revision of our manuscript entitled "2-photon imaging of microglial processes attraction toward ATP or serotonin in acute brain slices ~~of young and adult mice~~", by F. Etienne et al.

To address the comments of the editors and reviewers, which were very constructive and relevant, we made numerous revisions and thanks to that, we think that the manuscript is now much more precise and provides more useful indications for readers interested in doing live imaging on microglia. Notably, we added a figure (7B) and discussed more deeply our protocol in comparison with others, highlighting its strengths and limitations, and providing suggestions for improvements or application to other biological questions.

We therefore hope that our revised manuscript will fulfill the criteria of JoVE editorial board for acceptance and look forward recording the video.

Sincerely,

A handwritten signature in blue ink, reading 'ARoumier', is positioned above a short horizontal blue line.

Dr Anne Roumier

TITLE:

Two-photon Imaging of Microglial Processes' Attraction Toward ATP or Serotonin in Acute Brain Slices

AUTHORS & AFFILIATIONS:

Fanny Etienne^{1,2,3}, Vincenzo Mastrolia^{1,2,3}, Luc Maroteaux^{1,2,3}, Jean-Antoine Girault^{1,2,3}, Nicolas Gervasi^{1,2,3} *, Anne Roumier^{1,2,3} *

¹Institut national de la santé et de la recherche médicale (INSERM), Institut du Fer-à-Moulin (UMR-S 839), Paris, France

²Sorbonne Université, Paris, France

³Institut du Fer à Moulin, Paris, France

* These authors contributed equally.

Corresponding Authors:

Anne Roumier (anne.roumier@inserm.fr)

Phone: +33 1 45 87 61 24

Nicolas Gervasi (nicolas.gervasi@inserm.fr)

Phone: +33 1 45 87 61 53

E-mail Addresses of the Co-authors:

Fanny Etienne (Fanny.etienne@inserm.fr)

Vincenzo Mastrolia (Vincenzo.mastrolia@inserm.fr)

Luc Maroteaux (Luc.maroteaux@inserm.fr)

Jean-Antoine Girault (Jean-antoine.girault@inserm.fr)

KEYWORDS:

Microglia, multi-photon microscopy, acute brain slices, chemoattraction, motility, morphology, serotonin, ATP, live imaging, time-lapse imaging

SUMMARY:

Microglia, the resident immune cells of the brain, respond quickly with morphological changes to modifications of their environment. This protocol describes how to use two-photon microscopy to study the attraction of microglial processes toward serotonin or ATP in acute brain slices of mice.

ABSTRACT:

Microglial cells are resident innate immune cells of the brain that constantly scan their environment with their long processes and, upon disruption of homeostasis, undergo rapid morphological changes. For example, a laser lesion induces in a few minutes an oriented growth of microglial processes, also called "directional motility", toward the site of injury. A similar effect can be obtained by delivering locally ATP or serotonin (5-hydroxytryptamine [5-HT]). In this

article, we describe a protocol to induce a directional growth of microglial processes toward a local application of ATP or 5-HT in acute brain slices of young and adult mice and to image this attraction over time by multiphoton microscopy. A simple method of quantification with free and open-source image analysis software is proposed. A challenge that still characterizes acute brain slices is the limited time, decreasing with age, during which the cells remain in a physiological state. This protocol, thus, highlights some technical improvements (medium, air-liquid interface chamber, imaging chamber with a double perfusion) aimed at optimizing the viability of microglial cells over several hours, especially in slices from adult mice.

INTRODUCTION:

Microglial cells are the brain's resident macrophages and play a role in both physiological and pathological conditions^{1,2}. They have a highly branched morphology and are constantly extending and retracting their processes^{3,4}. This "scanning" behavior is believed to be related and necessary to the survey of their surroundings. The morphological plasticity of microglia is expressed in three modes. First, some compounds rapidly modulate microglial morphology: the addition of ATP^{5,6} or NMDA^{5,7} in the medium bathing acute brain slices increases the complexity of microglial ramifications, whereas norepinephrine decreases it⁶. These effects either are directly mediated by microglial receptors (for ATP and norepinephrine) or require an ATP release from neurons (for NMDA). Second, the growth and retraction speed of microglial processes, called motility or "surveillance", can be affected by extracellular factors⁸, homeostasis disruptions^{9,10}, or mutations⁹⁻¹¹. Third, in addition to these isotropic changes of morphology and motility, microglia have the capacity to extend their processes directionally toward a pipette delivering ATP^{3,5,12-14}, in culture, in acute brain slices or *in vivo*, or delivering 5-HT in acute brain slices¹⁵. Such oriented growth of microglial processes, also called directional motility, was first described as a response to a local laser lesion^{3,4}. Thus, physiologically, it may be related to the response to injury or required for targeting microglial processes toward synapses or brain regions requiring pruning during development^{15,16}, or in physiological¹⁷⁻¹⁹ or pathological situations^{9,18-20} in adulthood. The three types of morphological changes rely on different intracellular mechanisms^{11,13,20}, and one given compound does not necessarily modulate all of them (*e.g.*, NMDA, which acts indirectly on microglia, has an effect on morphology but does not induce directional motility^{5,7}). Therefore, when aiming to characterize the effect of a compound, a mutation or a pathology on microglia, it is important to characterize the three components of their morphological plasticity. Here, we describe a method to study the directional growth of microglial processes toward a local source of compound, which is, here, ATP or 5-HT.

There are several models to study microglia processes' attraction: primary cultures in 3D environment^{6,18,19}, acute brain slices^{6,13,15}, and *in vivo* imaging^{3,13}. The *in vivo* approach is the best to preserve the physiological state of microglia. However, intravital imaging of deep regions requires complex surgical procedures and, therefore, it is often limited to superficial cortical layers. The use of microglia primary culture is the easiest technique to test a large number of conditions with a limited number of animals. Nevertheless, it is impossible to obtain the same cell morphology as *in vivo*, and cells lose their physiological interactions with neurons and astrocytes. Acute brain slices represent a compromise between these two approaches. This model allows researchers to study brain structures which are otherwise difficult to reach and to

image with high resolution *in vivo*, and to investigate slices from neonatal stages, whereas transcranial microscopy is mostly performed at adulthood. Finally, it makes it possible to observe in real-time the effects of local drug application, and to repeat experiments while using a limited number of animals. Nonetheless, an issue with acute brain slices is the limited time (a few hours) during which the cells remain alive, notably for slices from mice older than two weeks, and the potential change of microglia morphology over time^{21,22}.

Here, we describe a protocol to prepare acute brain slices of young and adult Cx3cr1^{GFP/+} mice up to two months old, with the preservation of microglia morphology and motility for several hours. We, then, describe how to use these slices to study the attraction of microglial processes toward compounds like ATP or 5-HT.

PROTOCOL:

All experiments were approved by the local ethical committee (Darwin Committee, agreements #1170 and #10921).

1. Preparation of Glass Micropipettes for the Local Application of Compounds

1.1. Prepare pipettes from borosilicate thin-wall glass capillaries with an electrode puller. Adjust the parameters to obtain pipettes with a 4 - 5 μm diameter at their extremity. **Figure 2D** shows one pipette in brightfield at low magnification.

2. Solutions

2.1. Ensure that only glassware that has been cleaned by an autoclave cycle, followed by rinsing 2x - 3x with ultrapure water, will be used. Never use glassware that has been in contact with paraformaldehyde.

2.2. Prepare a 2 mol·L⁻¹ CaCl₂ stock solution by dissolving 14.7 mg of CaCl₂·2H₂O in 50 mL of water of high purity (ultrapure water, resistance 18.2 M Ω ; the traces of metal in distilled water or tap water can lead to suboptimal slice quality due to pro-oxidative effects).

2.2.1. Store this stock solution at room temperature for a maximum of one month.

2.3. On the day of the experiment, prepare 1 L of choline-aCSF (artificial cerebrospinal fluid) solution, whose composition is 110 mmol·L⁻¹ choline Cl, 25 mmol·L⁻¹ glucose, 25 mmol·L⁻¹ NaHCO₃, 7 mmol·L⁻¹ MgCl₂, 11.6 mmol·L⁻¹ ascorbic acid, 3.1 mmol·L⁻¹ sodium pyruvate, 2.5 mmol·L⁻¹ KCl, 1.25 mmol·L⁻¹ NaH₂PO₄, and 0.5 mmol·L⁻¹ CaCl₂, 0.5.

2.3.1. To prepare this solution, add, in the following order, to a 1 L graduated flask: 0.186 g of KCl, 0.195 g of NaH₂PO₄, 2.04 g of acid ascorbic, 2.1 g of NaHCO₃, and 4.5 g of glucose.

2.3.2. Fill about half of the final volume with ultrapure water and stir until complete dissolution.

2.3.3. Add 0.34 g of sodium pyruvate and 15.36 g of choline Cl.

NOTE: It is convenient to first dissolve the choline Cl with 5 to 10 mL of the solution prepared in step 2.3.2 before adding it to the whole solution.

2.3.4. Add 7 mL of 1 mol·L⁻¹ MgCl₂ and 250 µL of 2 mol·L⁻¹ CaCl₂ (prepared in step 2.2) to the solution.

2.3.5. Fill the graduated flask up to 1 L with ultrapure water.

2.3.6. With a vapor pressure osmometer, check that the osmolarity is between 300 and 310 mΩ. If not, adjust it with glucose.

2.3.7. Check the pH after carbogenation (*i.e.*, bubbling with “carbogen”, a mix of 95% O₂/5% CO₂) and adjust it, if necessary, to 7.3 - 7.4 with 10 M NaOH.

2.3.8. Transfer the solution to a glass bottle for storage. Keep the bottle in the fridge until use (STEP 3.1).

NOTE: It is recommended to make a fresh solution on the day of the experiment. However, if necessary, choline-aCSF can be stored up to two days at 4 °C.

2.4. On the day of the experiment, prepare 1 L of an aCSF solution, whose composition is 124 mmol·L⁻¹ NaCl, 26.2 mmol·L⁻¹ NaHCO₃, 25 mmol·L⁻¹ glucose, 2.5 mmol·L⁻¹ KCl, 2 mmol·L⁻¹ CaCl₂, 1 mmol·L⁻¹ MgCl₂, and 1.25 mmol·L⁻¹ NaH₂PO₄.

2.4.1. To prepare this solution, add, in the following order, to a graduated flask: 0.150 g of NaH₂PO₄, 0.186 g of KCl, 2.2 g of NaHCO₃, 4.5 g of glucose, and 7.3 g of NaCl. Bring the solution to a volume of 1 L with ultrapure water and stir it vigorously on a stir plate.

2.4.2. Add 1 mL of 1 mol·L⁻¹ MgCl₂ and 1 mL of 2 mol·L⁻¹ CaCl₂ to the solution and transfer the aCSF solution to a glass bottle for storage.

2.4.3. Check whether the osmolarity is 300 - 310 mΩ·L⁻¹ and, if not, adjust it with glucose.

2.4.4. Check the pH after carbogenation (*i.e.*, bubbling with “carbogen”) and adjust it, if necessary, to 7.3 - 7.4 with 10 M NaOH.

2.4.5. Transfer the solution to a glass bottle for storage. Keep the bottle in the fridge until use (step 3.1).

NOTE: It is recommended to make a fresh solution on the day of the experiment. However, an alternative is to prepare a 10x stock solution containing NaCl, NaHCO₃, KCl, and NaH₂PO₄ at 10x the final concentration, which can be stored for no more than one week at 4 °C. Make the final

aCSF on the day of the experiment by diluting the 10x stock solution with ultrapure water and adding the glucose, CaCl_2 , and MgCl_2 .

2.5. Prepare the drug solutions on the day of the experiment. Use the aCSF solution to bring them to the final concentrations which are, here, $500\ \mu\text{mol}\cdot\text{L}^{-1}$ for ATP and $5\ \mu\text{mol}\cdot\text{L}^{-1}$ for 5-HT.

NOTE: For ATP, a stock solution can be prepared (*e.g.*, 50 mM ATP in water), stored in aliquoted form at $-20\ ^\circ\text{C}$, and diluted with aCSF to the final concentration on the day of the experiment. In contrast, the 5-HT (serotonin-HCl) solution must be prepared from powder on the day of the experiment, at $1\ \text{mg}\cdot\text{mL}^{-1}$ in water, kept at $4\ ^\circ\text{C}$ to avoid 5-HT oxidation, and diluted in aCSF at the time of the experiment.

3. Preparation of Acute Brain Slices

3.1. Preparation of the dissection area

3.1.1. Prepare 70 mL of ice-cold choline-aCSF in an 80 mL beaker placed on ice, to be used for cardiac perfusion, rapid cooling down of the brain, and slicing. Prepare 150 mL of choline-aCSF in a 200 mL crystallizing dish, placed in a heated water bath maintained at $32\ ^\circ\text{C}$. Place a nylon mesh strainer in the crystallizing dish to retain the slices. This will be used to let the slices recover for 10 min just after slicing.

3.1.2. At least 30 min before starting the dissection (section 3.2), start bubbling these two solutions (70 mL of choline-aCSF on ice and 150 mL of choline-aCSF at $32\ ^\circ\text{C}$) with carbogen. Maintain constant carbogenation during the entire procedure.

3.1.3. Prepare the interface chamber device (**Figure 1C**), which will be used to keep slices until their use.

3.1.3.1. In a sealed food box (10 x 10 cm or 10 cm in diameter, 8 cm in height), installed on a magnetic stirrer, place a 200 mL crystallizing dish with a bar magnet.

3.1.3.2. Add 200 mL of aCSF in this crystallizing dish and place the 3D-printed interface slice holder on top of it (the interface slice holder is composed of two perfectly fitting parts, with a polyamide mesh stretched between them, **Figure 1A,B**).

3.1.3.3. Remove excess volume from the crystallizing dish to keep only a thin film of solution covering the mesh of the interface slice holder. This will later create a fine rim of solution surrounding the slices (but without covering them).

3.1.3.4. Put a few millimeters of aCSF at the bottom of the food box and start bubbling it with carbogen (at first use, make a small hole in the sealed food box wall to make sure the tubing can enter the box).

3.1.3.5. Close the sealed box while maintaining constant carbogenation. This will create a humidified 95% O₂/5% CO₂ rich environment in which the slices will be transferred after their recovery in choline-aCSF and maintained before they are imaged. This device is hereafter referred to as the “interface chamber” (Figure 1C).

3.2. Brain dissection and slicing

3.2.1. Anesthetize the mouse with an intraperitoneal injection of 50 mg·mL⁻¹ pentobarbital (0.15 mL/20 g of mouse body weight), immobilize it, expose the heart, and perform a cardiac perfusion with 10 mL of ice-cold, carbogenated, choline-aCSF (see step 3.1.1), with a peristaltic pump. Observe the pallor of the liver as an indicator of a good perfusion. The perfusion lasts less than 5 min.

3.2.2. Decapitate the mouse and cut the skin to expose the skull. With big scissors, apply two transversal cuts from the large foramen and one long sagittal cut and, using fine forceps, remove the skull plates.

3.2.3. Quickly and gently extract the brain (in less than 1 min) and place it for 1 min in the 80 mL beaker containing the remaining (~60 mL) ice-cold choline-aCSF (still under constant carbogenation), in order to cool it down.

3.2.4. Transfer the brain onto a filter paper previously wet with aCSF.

3.2.5. Cut out the brain according to the brain region of interest and preferred angle of slicing. For example, to image the thalamus or the hippocampus on coronal slices, cut out with a scalpel blade the cerebellum and, then, about 2 mm from the rostral and caudal extremities of the brain.

NOTE: It is important to remove brain parts that are too rostral or too caudal because the smaller the region to trim before reaching the area of interest, the faster the slicing. A total time for slicing (step 3.2.7) of less than 20 min is recommended.

3.2.6. For coronal slices, position and glue (with cyanoacrylate glue) the caudal face of the brain onto a 10 cm Petri dish, glued on the cutting block and filled with all the remaining ice-cold choline-aCSF. The block with the dish is, then, positioned in the reservoir chamber of the vibrating slicer, which is positioned in a larger chamber filled with ice.

3.2.7. While keeping constant the 95% O₂/5% CO₂ bubbling of the ice-cold choline-aCSF, cut 300 µm-thick coronal slices (speed: 0.08 mm·s⁻¹, blade vibration: 60 Hz, vibration amplitude: 1 mm).

3.2.8. Collect the brain slices with a wide-mouth (4 mm in diameter) disposable transfer pipette, one by one after every single pass of the blade, to avoid the accumulation of toxic components released by the periphery of the slices. Take care to avoid air bubbles during the transfer and place each slice in the choline-aCSF at 32 °C for about 10 min for recovery.

3.2.9. With the transfer pipette, place the slices onto pieces of lens-cleaning paper topped with a drop of choline-aCSF. Aspirate the excess of choline-aCSF and, with the spatula, place the slices, laid on the lens-cleaning tissue, on the mesh of the interface chamber containing carbogenated aCSF at room temperature (see 3.1.3.5). Let the slice recover in this environment for at least 30 min.

NOTE: After this, the slices are ready and can be used for microglia imaging for up to 6 h after the brain extraction from young (less than one-month-old) mice and up to 4 h after the brain extraction from two-months-old adults.

4. Two-photon Microscopy

4.1. Parameters setting

4.1.1. Switch on the multiphoton system (hybrid detectors, laser, scanner, electro-optic modulator, microscope).

4.1.2. Tune the laser at 920 nm, check that the laser is mode-locked, and set the power at 5% - 15% and the gain at 10%. This corresponds to a power of 3 - 5 mW under the objective. Ensure that the nondescanned detectors are engaged and the appropriate emission and excitation filters installed.

4.1.3. Set parameters of the imaging software to the following values: for the frame size, 1024 x 1024 pixels corresponding to an area of 295.07 x 295.07 μm ; for the zoom, 2. If the signal is very noisy, apply a line average of 2. For the pixel dynamics, set the imaging software at 12 bits or more.

NOTE: Images with a higher bit value allow researchers to distinguish smaller differences in fluorescence intensity than images with a lower bit value: a change of one gray value in an 8-bit image would correspond to a change of 16 gray values in a 12-bit and of 256 gray values in a 16-bit image. Therefore, higher-bit images are more appropriate for quantitative analysis, but as their size increases with bit depth, storage capacity, and computing power can become limiting.

4.1.4. Select the scan mode XYZT with a Z-interval range at 2 μm and a T-interval of 2 min.

NOTE: The x,y and z resolution are determined by the Nyquist sampling theorem. A Z-step size around 0.8 would be optimal to resolve microglia processes (with a diameter of <1 μm), but the optical resolution of multiphoton microscopy is limiting (at 920 nm with a 0.95 NA objective, the axial resolution is around 1 μm). On top of that physical barrier, in a live-imaging experiment, the sensitivity or signal-to-noise ratio, the resolution, the speed, and the total observation time matter. Taking into account all these parameters, a z-step of 2 μm (as in numerous studies^{3,11,14}), an image size of 1024 x 1024 pixels, and a high-speed acquisition using a resonant scanner coupled to HyD detectors (it takes around 15 s to acquire 50 z-plans) were selected here. The frequency of acquisitions is one XYZT series every 2 min and the total duration is 30 min. If the

set-up is not fast or sensitive enough, it is possible to reduce the lateral resolution (down to 512 x 512) or the number of z-slices (by imaging exclusively in the z-depth which exhibits the strongest fluorescence [*i.e.*, not the deepest z-slices where fluorescence is faint]), or to decrease the speed of the scanner. The axial resolution can also be decreased by increasing the z-step up to 3 μm , but as this may impact the quantification, all experiments to be compared should be performed with the same z-step.

NOTE: It is possible to perform similar experiments on slices from CX3CR1creER-YFP mice¹⁸, a mouse line used to induce genetic deletion in microglia only, and in which microglia constitutively express yellow fluorescent protein (YFP). However, the expression level of YFP is very low compared to green fluorescent protein (GFP) in CX3CR1^{GFP/+} mice; thus, imaging is possible but challenging and requires the optimization of the acquisition parameters. It is recommended to adjust them as follows.

4.1.5. Tune the laser at 970 nm (which is better adapted to YFP excitation than 920 nm), the power at 50%, and the gain at 50%, which corresponds to a laser power under the objective of 5 - 6 mW.

4.1.6. Set a line average of 4 (or more) to improve the signal-to-noise ratio.

4.2. Positioning of the slice and of the glass micropipette, and the local application of the compound

4.2.1. Connect the peristaltic pump to the recording chamber, 30 min before starting the recording. After cleaning the whole perfusion system with 50 mL of ultrapure water, start the perfusion of the recording chamber with aCSF (50 mL) contained in a glass beaker under constant carbogenation. Throughout the experiment, keep the circulating aCSF to 32 °C with an inline microheater or a Peltier heater.

NOTE: A specific perfusion chamber with top and bottom perfusion is designed to optimize the oxygenation on both sides of the slice. The perfusion chamber is composed of two perfectly fitting parts, with a polyamide mesh stretched between them (**Figure 2A,B**). Compared with other types of chambers, where the slice is directly laying on a glass coverslip, this chamber reduces neuronal death in the bottom part of the slice, improves viability, and reduces the slice movements induced by its swelling.

4.2.2. With a wide-mouth disposable transfer pipette, transfer the brain slice to be imaged to the aCSF beaker to remove the lens paper, let it sink (as a proof that no air bubble is attached), and transfer it to the recording (perfusion) chamber.

4.2.3. Position a slice holder (a hairpin made of platinum with the two branches joined by parallel nylon threads) on the slice to minimize slice movement due to the perfusion flow.

4.2.4. Use the bright-field illumination to target the brain region of interest (exposure time: 50 to 80 ms) using a low magnification objective (5X or 10X). Switch to the higher magnification (25X with a 0.35X lens) water immersion objective and adjust the position.

NOTE: Avoid to image fields close to the slice holder's nylon threads as they can block the light and locally deform the slice. Make sure that the area of interest is flat. If necessary, remove the slice holder in order to reposition the slice and/or the slice holder.

4.2.5. Use the fluorescence illumination to locate fluorescent microglial cells to be imaged in the field (exposure time: 250 - 500 ms).

NOTE: This step allows researchers to check the presence of cells in the region of interest and their fluorescence intensity, and to control for the amount of cellular debris.

4.2.6. Backfill the pipette with 10 μ L of aCSF with ATP, 5-HT, or the drug of interest at its final concentration. Point the tip downward and gently shake the drug-filled pipette to remove any air bubbles trapped in the tip.

NOTE: If the solution to be injected tends to form bubbles, consider using borosilicate pipettes with an internal filament. Leakage of ATP out of the pipette can attract microglial processes even before the injection (if this occurs, it will be visible at the analysis step). Although this should be moderate with the ATP concentration used ($500 \mu\text{mol}\cdot\text{L}^{-1}$), if it is an issue, consider prefilling the micropipette with 2 mL of aCSF prior to adding the ATP (or other compound) solution at step 4.2.6.

4.2.7. Mount the filled pipette in a pipette holder, connected with transparent tubing to a 5 mL syringe, with a plunger positioned at the 5 mL position. The pipette holder itself is mounted onto a three-axis micromanipulator.

4.2.8. Under bright-field illumination, use the micromanipulator to position the pipette in the center of the field. For a reproducible and optimal centering, display and use the rulers on the image.

4.2.9. Lower the pipette gently toward the slice, controlling and adjusting the objective at the same time, until the pipette tip lightly touches the surface of the slice. Stopping the descent of the pipette as soon as it is visible that the slice has been touched allows the pipette tip to penetrate 80 - 100 μm of the surface of the slice (see **Figure 3B**).

4.2.10. Tune the laser (see the parameters above) and switch the microscope to the multiphoton mode. Make sure that the chamber is screened from any light source (e.g., a computer screen). Switch on the nondescanned detectors and set the gain. Use a lookup table (LUT) with a color-coded upper limit to avoid saturating the pixels in the image.

4.2.11. Determine the thickness of the slice to be imaged (*i.e.*, the upper and lower z-positions where fluorescence is detectable [usually between 220 and 290 μm in total]).

NOTE: At the surface of the slice, there is an increased density of processes and possibly of microglia, often with an unusual morphology, in comparison with the inside of the slice. This accumulation will be more striking with time (*i.e.*, more visible in the last than in the first brain slice to be imaged). Therefore, the z-planes in the first $\sim 30\ \mu\text{m}$ should not be used for the analysis and can even be skipped for the acquisition.

4.2.12. Start recording for a total duration of 30 min (or more if desired) and after a 5 min baseline, locally apply the compound to be tested (without interrupting the imaging). To do this, slowly press the plunger of the syringe connected to the micropipette, from the 5 mL to the 1 mL position (in about 5 s). Resistance when pressing the plunger must be felt immediately. If not, the tip might be broken.

NOTE: For a trained experimenter, the injections with this method are reproducible, but alternatively to the manual manipulation of a syringe, the pipette could be linked to an automated pressure ejection system to allow a better control of the volume delivered. The injection creates a physical distortion of the slice at the site of the injection. This distortion is visible *a posteriori* in the first two or three images after the injection but should not be visible on the fourth image, (*i.e.*, 8 min after the injection). If it persists, consider changing the parameters for the pipette preparation.

4.2.13. At the end of the acquisition (30 min), discard the micropipette and remove the slice. If desired, fix the slice for further immunolabeling. For example, the SNAPSHOT method is optimized for the fixation and staining of thick slices²³.

4.2.14. Prior to starting to image a new slice, make the 2D movie (section 5.1) in order to check that microglia have a normal morphology and are moving and, thus, that the slices are healthy.

5. Analysis of the Attraction of Microglial Processes

5.1. 2D projection and drift correction

5.1.1. Open the file (.LIF) with Fiji²⁴.

5.1.2. If necessary, make a substack (**Image/Stacks/Tools/Make Substack**) with only the z-planes of interest. For example, exclude the z-planes corresponding to the surface of the slice if they have been acquired but are not to be used for the analysis (see the NOTE after step 4.2.11) and the deepest z-planes with no fluorescence. The final stack generally contains 90 - 110 z-slices (180 - 220 μm).

5.1.3. Launch the **Z project** function (**Image/Stacks/Z Project**) and select the **Max Intensity** projection type to make the projections of the z-stack acquired at each time point.

5.1.4. Launch the **MultiStackReg** plugin (**Plugin/Registration/MultiStackReg**), selecting **Action 1: Align** and **Transformation: Rigid Body** to correct slight drifts that may have occurred during the acquisition. Save this 2D movie as a new file (.TIFF).

5.2. Data processing

5.2.1. Open this new file with Icy²⁵.

5.2.2. Draw a circular **R1** region of interest (ROI) of 35 µm in diameter, centered on the injection site (identified notably by the shadow of the pipette and the distortion created at the time of injection).

5.2.3. Use the plugin **ROI intensity evolution** and measure the mean intensity over time in R1.

5.2.4. Save the results to an .XLS file.

5.3. Quantification and representation of the results

5.3.1. To quantify the microglial response over time, determine at each time point

$$R(t) = \frac{[R1(t) - \bar{R1}(0)]}{\bar{R1}(0)}$$

Here, $\bar{R1}(0)$ is the mean of the $R1(t)$ values before the injection. Then, the results can be represented as a kinetic of the microglial response, or at a specific time point (see **Figure 7**).

REPRESENTATIVE RESULTS:

This protocol describes a method to induce, observe, and quantify the oriented growth of microglial processes toward a locally applied compound, for example, ATP or 5-HT, in acute brain slices from young or adult (at least up to two-month-old) mice. Among the factors that contribute to maintaining brain slices from adult animals in a healthy state for several hours is the use of two tools designed to optimize cell survival at two steps of the protocol. First, the interface slice holder in the interface chamber (**Figure 1**) improves the conservation of the slices after cutting. Second, the recording chamber (**Figure 2**) has a perfusion system which allows the aCSF to run both at the top and at the bottom of the slice during imaging. The recording chamber dimensions used here are set to fit standard microscopes as they are similar to classical bath chamber inserts (with a 62 mm outer diameter), but as their models are downloadable from the **Supplemental Material**, the design can be adapted to fit in slice holders of other dimensions. To note is that each chamber is made by the assembly, without glue, of two perfectly fitting parts, with a polyamide mesh stretched between them.

To deliver ATP or 5-HT in a small area and induce a local response of microglia, a pipette containing the compound (visible in **Figure 2C,D**) is placed with its tip on top of the slice. In the first experiments, it can be helpful to add a fluorescent dye to the solution, in order to visualize the position of the pipette tip on the images that are acquired with the two-photon microscope (**Figure 3A**). In **Figure 3B**, it is visible that although the experimenter stopped the pipette descent as soon as its tip touched and deformed the slice surface on the bright-field image of the computer screen, its thin extremity entered slightly into the tissue, down to 80 - 100 μm from the surface. It is important that the pipette is not too superficial because it may not deliver the solution correctly onto the cells, nor enter too deep because it may reach a region where the fluorescence signal is too low. The parameters that may affect the depth reached by the pipette tip are the angle of the pipette, which can be adjusted with the three-axis micromanipulator, and the pipette mouth diameter.

Note that, with the projection along the Y-axis (**Figure 3B**), it is possible to observe that the fluorescence is stronger in the upper than in the lower part of the slice. This is due both to the progressive blunting of the signal inside the slice and to the fact that processes of microglia of the superficial layers of the slice, and some cell bodies, tend to migrate toward the surface. As a result, microglia in the most superficial layers of the slice might show a different morphology than those inside the slice, indicating that they are not in the same state, and may react differently to stimulation. Thus, superficial microglial activation may mask, in the z-projection, the response of the microglia below. In addition, the surface is often tilted, and the first z-images of the stacks are patchy. Therefore, we recommend, for a better accuracy, to exclude the most superficial z-planes from the z-projection and analysis. However, as altered microglia morphology and the presence of debris in the superficial layers are indicators of the condition of the slice, it can be interesting to image the full depth of a slice to check its status *a posteriori*. This can be especially useful to new experimenters who may not easily recognize abnormal microglia or debris from single z-planes. The z-planes taken in the first 30 μm will then be excluded at the z-projection step (step 5.1.2 of the protocol).

Once the slice has been treated with the compound of interest and recorded, the series of z-planes (excluding the first 30 μm , as discussed above) imaged at each time point are projected along the z-axis to make a 2D movie of z-projection images. To note is that in the protocol presented here, the thickness used for the max z-projection encompasses all the z-slices where fluorescence is visible (usually 180 - 220 μm , see step 5.1.2 of the protocol). Therefore, variations in the absolute number of z-slices do not impact the quantification of the response. In contrast, some studies use thinner z-stacks (40 - 60 μm) for z-projection^{6,7,11,27}. This is another option, which comes with the risk to exclude some z-slices which exhibit a response, as we observed that the attractant effect was visible as far as 70 μm (in z) away from the pipette tip in some experiments. If the thinner option is preferred, it is, thus, critical to center the z-stack on the pipette tip in z, and importantly, only z-projections done in the same manner (*i.e.*, using all fluorescent z-slices or using a thin z-stack) can be compared.

An R1 region of interest is then defined for quantitative analysis. **Figure 4** shows an ROI on a z-projection. The red dashed lines represent the putative position of the pipette. The yellow circle

is R1, drawn with Icy, and centered on the putative tip of the pipette. Importantly, we observed that a noticeable variability arose during the quantification from the localization of the R1 ROI, whose misplacement leads to an underestimation of the response. To help positioning the ROI on the site of delivery, we recommend displaying the rulers in the acquisition software when positioning the pipette in the brightfield, in order to place the pipette tip always in the same central XY position in the field to be imaged. This provides an indication of where to position, later, the ROI in the Z-projection of the fluorescence images. However, the final tip position and, thus, the actual site of delivery will be slightly shifted from this central position, depending on the depth reached by the pipette tip. For this reason, to position R1, we take into consideration three other criteria: (i) R1 must be at the tip of the pipette, the position of which is inferred from the dark background in the lower right corner, (ii) it should correspond to the area where a transient distortion of the tissue occurs when the compound is injected, and (iii) it should correspond to the area where a local response (if any) is observed. If this is not sufficient to locate with good accuracy the point of delivery, filling the pipette with a fluorescent compound will help. After having drawn R1, we run the movie again to check that it is well positioned for all the time points and that there are no aberrant drift, distortion, or artifact fluorescence at any time point, which could bias the quantification. The movie corresponding to **Figure 4**, and illustrating the effect of ATP application, can be found in the supplemental material (**Movie S1**).

We initially studied the attraction of microglial processes toward ATP or 5-HT in the thalamus of P11 mice¹⁵. More recently, these experiments were repeated in slices from four-day- to two-month-old mice, and in various regions (for example, **Figure 3** corresponds to a recording in the hippocampus). We mostly used three- to four-week-old mice, which combines the advantages of having a mature brain—with mature and ramified microglia—with a good slice viability. Importantly, representative normal-state microglia are characterized by a small soma, long processes with small terminals, and constantly moving processes at the baseline condition. Typically, in slices from 18- to 30-day-old mice, the microglia morphology remains mostly unchanged for up to 6 h after the slice preparation. For slices from older mice (two months old), the ability to maintain the slices in a physiological state is reduced (~4 h). Examples of microglial direction motility in the thalamus, in response to 5-HT in a slice from a 20-day-old mouse and to ATP in a slice from a two-month-old mouse, are provided in **Figure 5**. The movie corresponding to the 5-HT application in **Figure 5** can be found in the supplemental material (**Movie S2**).

Figure 6 presents two suboptimal experiments made on slices kept for longer than 6 h in aCSF before they were imaged (only times 0 are shown). In **Figure 6A**, note the presence of microglia with multiple short processes or with enlarged terminals reminiscent of neurite growth cones, and the presence of many fluorescent cell debris or particles. These very fluorescent elements stay immobile or move randomly during imaging, indicating that they do not belong to “living” microglia (see **Movie S3** in the supplemental material). To note is that, in this particular example, microglia were constantly scanning their environment, but their morphology was so altered that they could not be considered as being in a physiological state. Moreover, the large amount of debris would have made the fluorescence analysis poorly reliable. **Figure 6B** illustrates the presence of microglia with large and flat cell bodies or protrusions, which can sometimes be found on the superficial layers of slices that have been kept several hours before they were

imaged. Only superficial z-positions have been used to make this z-projection. **Figure 6C** is a substack, at deeper z-positions, from the same brain slice as shown in **Figure 6B**. Although they are not positioned at the surface, these microglia have an abnormal “bushy” aspect. Due to the aspect of microglia, the movies corresponding to these two slices were not used for quantification.

After extracting the data from the 2D-movies, the results can be represented by plotting normalized $R(t)$ fluorescence over time. A graph summarizing several experiments is presented in **Figure 7A**, to show the variability of the responses. Note that the fluorescence decreases immediately but transiently (in the first three images) after the injection due to tissue distortion (*i.e.*, the liquid injection with the pipette transiently pushes the tissue away, and then increases). The variability in the response to ATP illustrates the fact that even when slices look similarly healthy, with motile and ramified microglia, they do not respond in the same manner (but all of them do respond). On top of intrinsic sample heterogeneity, there is some looseness in the R1 positioning, as mentioned above, and we also cannot exclude an impact of, for example, differences in the volume of the solution which is delivered. Therefore, to detect small effects or variations, it may be interesting to use an automatic device for the compound injection.

Figure 7B shows how the size of the ROI also impacts the quantification, here of the growth of ATP-induced processes. Increasing the diameter from 35 (the diameter used in **Figure 7A** and for all the analyses presented here) to 50 or 70 μm reduces the variability among experiments (slices) by suppressing the issue of the small R1 positioning. However, it also decreases accuracy and the magnitude of the detected response. Indeed, with larger ROIs, there is more background due to processes or cell bodies not affected by the treatment, and a growth of processes can be partially blunted by the concomitant retraction of microglial branches more distant from the pipette but nevertheless inside the ROI. In conclusion, it can be relevant to use ROIs with a different diameter circle than one that is 35 μm , but it is fundamental that the ROI is always the same in all the data sets to be compared.

Figure 7C shows the mean \pm SEM for several experiments with aCSF, ATP, or 5-HT. The effect of ATP is in the same range as those obtained by other groups with a similar method *in vivo* (0.5 according to Davalos *et al.*³ and 0.4 according to Haynes *et al.*¹³) and in slices (0.8 if normalized as is done here, according to Dissing-Olesen *et al.*⁵, and 0.6 according to Pagani *et al.*²⁸). On the one hand, differences can come from biological parameters, such as the slice preparation method, the amount of ATP injected, the age of the mouse, or the brain region used, and on the other hand from analysis parameters, such as the diameter of the ROI and the thickness of the z-stacks used for the z-projection (*i.e.*, the whole thickness where fluorescence is detected, or only the 40 - 60 μm around the pipette tip, where the maximal response is expected).

In **Figure 7C**, the aCSF injection is the negative control, necessary to check that the local injection and the pressure of the pipette do not cause an injury that may attract microglial processes. In addition, the aCSF control allows researchers to check that there is no photobleaching over time. Indeed, photobleaching, the photon-induced destruction of the fluorescent proteins or fluorophores, would have induced a progressive decrease of fluorescence over time. As it can bias

measurements, it is important to rigorously check that there is no photobleaching in the experimental conditions. To do this, it is recommended to acquire an XYZT series on a slice with GFP-expressing microglia, for 30 min (aCSF can be injected but, actually, no stimulation is needed), with the excitation and acquisition parameters set as in the experimental conditions. Then, a quantitative measure of the fluorescence over time in different regions of interest, including microglia cell bodies or processes, will reveal if there is a gradual loss in emission intensity, usually an exponential decay, indicating photobleaching. If this is the case, some adjustments can be performed: a realignment of the laser, a reduction of the laser power and an increase of the detector gain, a reduction of the number of z-planes, and an increase of the interval between them to limit illumination. Photobleaching is favored by high-power or long (ex: repeated illumination for line averaging) excitation; thus, researchers must pay attention to it if a sustained illumination is used to image cells with low fluorescence.

After the local injection of ATP or 5-HT, there is an increase of fluorescence in R1, which reaches a plateau (**Figure 7C**). In addition to kinetics, it can be interesting to compare the attraction at a stable endpoint. Here, we chose to represent the microglial response at $t = 26$ min (*i.e.*, 20 min after the injection) in **Figure 7D**. This is useful to statistically compare compounds, or to test the effect of antagonists which can be added in the bath (*i.e.*, in the perfusion solution, or together with the compound in the pipette [not shown]).

FIGURE LEGENDS:

Figure 1: Interface chamber details. (A) Outline for the 3D printing of the slice holder. The external diameter of the holder is 7 cm. (B) Interface slice holder with the nylon mesh (arrow) that allows researchers to keep slices at the liquid-air interface. (C) Interface chamber device that makes it possible to maintain the slices in a carbogenated (the arrow indicates the tubing for bubbling) and humidified environment before they are imaged.

Figure 2: Perfusion chamber details. (A) Outline for the 3D printing. The external diameter of the perfusion chamber is 5.9 cm. (B) The perfusion chamber with the nylon mesh (arrow) that supports the slice, prevents it from touching the slide below, and allows the aCSF to flow above and under it. (C) Picture of the assembly at the two-photon microscope. The micropipette which will deliver the compound locally is visible on the right (asterisk). (D) Pipette imaged in brightfield. The scale bar = 60 μm .

Figure 3: Position of the micropipette in the slice. Example of an acquisition of a stack of images (in the hippocampus of a 30-day-old animal) with a micropipette filled with fluorescein (1 μM). Fluorescein makes it possible to locate the pipette (asterisk) in the max projections along (A) the z-axis or (B) the y-axis. Note in panel B that, although fainter in fluorescence, there are also microglia below the pipette tip. In this illustrated example, the full stack, including the images taken in the most superficial part of the slice, has been used for the projections. The scale bar = 30 μm in panel A and as indicated (each graduation = 50 μm) in panel B. The z-thickness of the stack = 220 μm .

Figure 4: Positioning of R1, the ROI used for quantification. This figure shows three experimental time points of an experiment where ATP has been applied on a slice (from the thalamus of a 20-day-old animal), with drawings of the putative location of the pipette (red dashed line on the first time point) and the delineation of the R1 ROI. The scale bar = 30 μm . Note the darker area in the lower right corner, corresponding to the shade of the pipette, which interferes with illumination and imaging. Note, also, the small region of intense fluorescence at 25 min, which indicates the location of the pipette tip. The z-thickness of the stack = 220 μm .

Figure 5: Microglial responses. Responses to the local application of 5-HT (5 μM) on a brain slice from a 20-day-old mouse (left; the slice z-thickness = 220 μm) and of ATP (500 μM) on a slice from a two-month-old mouse (right; the slice z-thickness = 220 μm). The red dashed lines represent the pipette position. Both recordings have been done in the thalamus, and the upper 30 μm of the slices have been excluded. The images are taken before (upper row) and 25 min after (lower row) the injection. The scale bar = 30 μm .

Figure 6: Examples of suboptimal experiments. These slices have waited for more than 6 h before imaging and have been imaged since their upper surface. **(A)** Example of a z-stack with a lot of debris (roughly round, fluorescent particles, but with irregular borders; asterisks) and “bushy” microglia (arrows), that is, with numerous but short processes. Note the enlarged process terminals (arrowheads) which look like axonal growth cones. The z-thickness of the stack = 220 μm . The other two panels show two sub-stacks of the same slice, with **(B)** 1-30 z-planes (z-thickness = 59 μm) and **(C)** 30-120 z-planes (z-thickness = 180 μm). On the top planes (shown in panel **B**), in addition to the large process terminals and debris like in panel **A**, there are microglia with unusual large flat bodies or protrusions (stars). On the deeper planes (shown in panel **C**), there is no debris nor flat objects, but the cells are bushy (arrows) and the density is unusually high. Altogether, these observations indicate that the microglia are not in a normal state.

Figure 7: Quantification of the attraction of microglial processes. **(A)** Example of a series of experiments with ATP to illustrate variability. **(B)** Impact of the ROI size on the quantification. Each experiment shown in panel **A** (ATP injection) has been analyzed with an ROI of 35, 50, or 70 μm diameter. The mean \pm SEM of the fluorescence at each time point is shown for the different ROIs. **(C)** Summary of experiments with aCSF, 5-HT, and ATP. The aCSF injection has no effect on the location of microglial processes. ATP and 5-HT induce a localized growth of microglial processes toward the pipette, measured with the local increase of fluorescence. The mean \pm SEM are indicated. **(D)** Summary of microglial responses at $t = 20$ min postinjection (26 min from the beginning of recording). The mean \pm SEM are indicated. One-way ANOVA with Dunnett *post hoc* test is used. ** $p < 0.01$, *** $p < 0.001$ compared to the aCSF injection. For aCSF, $n = 7$; for ATP, $n = 8$; for 5-HT, $n = 6$. All these experiments were performed in the thalamus, but similar results can be obtained from the hippocampus or cortex. The z-thickness of the stacks used for z-projections and quantification = 180 - 220 μm . All measures except those in panel **B** have been done with a 35 μm -diameter ROI.

Movie S1: Example of the effect of a local ATP (500 μM) application. This experiment has been performed in the thalamus of a 20-day-old animal. Images from this movie have been used for

Figure 4. The scale bar = 30 μm .

Movie S2: Example of the effect of a local 5-HT (5 μM) application. This experiment has been performed in the thalamus of a 20-day-old animal. Images from this movie have been used for **Figure 5** (left). The scale bar = 30 μm .

Movie S3: Example of a suboptimal experiment in a slice having waited for more than 6 h before imaging. Note the presence of numerous debris which moves randomly over time and the unusual morphology of the microglia. An image from this movie is used as **Figure 6A**. The scale bar = 30 μm .

Supplementary File. Imaging chamber and Interface holding chamber

DISCUSSION:

By maintaining, unlike in dissociated or organotypic slice culture, a structural integrity with limited network adjustments, acute brain slices allow researchers to study microglia in their physiological environment. However, one of the major limitations is the fact that the slicing procedure creates injuries that can rapidly compromise the viability of neurons, particularly in the adult brain. As microglia are particularly reactive to cell damage, it is important to limit neuronal cell death as much as possible to preserve microglia close to their physiological state. This, in turn, contributes *via* a virtuous circle to a better general condition of the slice.

The protocol described in this article applies several improvements found in the literature for electrophysiology experiments, aimed at obtaining a better viability of the slices over several hours, especially from adult mice. To overcome the age-related disparity in slice viability, we substituted sodium with choline and used this choline-aCSF medium during the cardiac perfusion, slicing, and recovery phases. This brings the cell excitotoxicity to a minimum^{29,30}. It should be noted that, in addition to choline-aCSF, there are many other alternative aCSF recipes that are highly effective for neuronal preservation, like N-methyl-D-glucamine (NMDG)-aCSF³¹, which could also be interesting for microglial studies but have not been tested here. Another critical step in this procedure is the cardiac perfusion. By perfusing the animal with a cold choline-aCSF solution, containing low Na^+ , low Ca^{2+} , and high Mg^{2+} , a rapid decrease in body temperature is induced and the metabolic activity of the cells in the brain is lowered, thereby reducing the cellular stress caused by the cutting. Indeed, we observed that this approach offered more protection than simply removing the whole brain and submerging it in aCSF solution. Inspired by a protocol optimized for patch-clamp and optogenetic studies²⁹, we also used a “protective recovery” period immediately following the physical slicing, allowing the slices to recover from the trauma of slicing for 10 min in choline-aCSF at 32 °C. Afterward, slices were transferred into the interface holding chamber to recover for an additional minimum time of 30 min. The duration of this second recovery period could be optimized according to the brain area of interest, the Na^+ substitute, and the age of the animal, and it should last at least 1 h if electrophysiology has to be performed in parallel with imaging.

The maintenance of the slice in a healthy state before use and the perfusion during imaging are

also important parameters. Both the interface and the dual-perfusion chamber are widely established tools in electrophysiology. For example, the interface method has been used to improve the viability of hippocampal slices since 1995²⁶. Devices similar to the chambers used here are proposed by several companies but not yet commonly used for microglia imaging. We designed an interface holding chamber, where the slices lay on a net and are on the interface with a large reservoir of aCSF, delaying the cellular deterioration of the slices during prolonged incubation times. In the imaging chamber, we used a designed double-sided perfusion chamber which allows increased oxygenation of acute slice preparations, maintaining the cells in a healthy state during multiphoton microscopy. In contrast with the single perfusion, the double perfusion of submerged slices increases the viability of the cells, since oxygen, as well as other materials, can freely and effectively diffuse with a high flow rate from both sides of considerably thick slices.

This protocol is aimed at quantifying the global attractant effect of ATP or other compounds on microglial processes, and its quantification method is based on the one used in Davalos *et al.*³. It is possible to perform other kinds of analysis. For example, an alternative method, which does not depend on the fluorescence level of the microglial processes but requires more actions of the experimenter for the image analysis, is to measure the reduction of the empty space around the pipette tip after compound application^{11,32}. It is also possible to track the movement of the tip of individual microglial processes^{15,28}.

In addition, the isotropic motility or surveillance of microglia can also be registered in basal condition or upon the bath application of compounds of interest on the slices prepared with this protocol. However, to quantify the fast extension and retraction rates of microglial processes and detect potential variations, it would be relevant to increase the acquisition frequency. For example, Pagani *et al.* use a frequency of one image every 10 s²⁸.

Finally, recent publications described methods to quantify morphological changes or the motility of individual processes in three dimensions. For such analyses, although a z-step interval of 2 μm is enough for some programs²⁷, others require a better axial resolution (*i.e.*, a z-step of 0.4 μm according to Heindl *et al.*³³).

Here, we showed experiments on wild-type mice with an endogenous expression of GFP in microglia and with a mechanical application of compounds, but this protocol can be adapted to other fluorescent reporter proteins in microglia, like YFP¹⁸, or to the exogenous labeling of microglia with fluorescent isolectin^{11,34}. Finally, we have studied the outgrowth of microglial processes toward a local application of ATP or 5-HT in a wild-type normal environment, but this protocol could be used to test other compounds, other kinds of stimulation (*e.g.*, caged compounds), and to test how directional motility is affected by mutations, pharmacological agents, or pathological contexts.

ACKNOWLEDGMENTS :

This work has been supported in part by the Centre National de la Recherche Scientifique, the Institut National de la Santé et de la Recherche Médicale, the Sorbonne Université Sciences, and by grants from Sorbonne Universités-Pierre et Marie Curie University (Emergence-UPMC program

2011/2014), the Fondation pour la Recherche sur le Cerveau, the Fondation de France, the Fondation pour la Recherche Médicale “Equipe FRM DEQ2014039529”, the French Ministry of Research (Agence Nationale pour la Recherche ANR-17-CE16-0008 and the Investissements d'Avenir programme “Bio-Psy Labex” ANR-11-IDEX-0004-02) and a Collaborative Research in Computational Neuroscience program, National Science Foundation/French National Agency for Research (number : 1515686). All the authors are affiliated to research groups which are members of the Paris School of Neuroscience (ENP) and of the Bio-Psy Labex. F.E. is a Ph.D. student affiliated with Sorbonne Université, Collège Doctoral, F-75005 Paris, France, and is funded by the Bio-Psy Labex. V.M. is a post-doctoral fellow funded by the Collaborative Research in Computational Neuroscience program, National Science Foundation/French National Agency for Research (number: 1515686). The authors thank Marta Kolodziejczak who participated in the initiation of the project.

DISCLOSURES:

The authors have nothing to disclose.

REFERENCES:

1. Salter, M. W., Stevens, B. Microglia emerge as central players in brain disease. *Nature Publishing Group*. **23** (9), 1018-1027, doi:10.1038/nm.4397 (2017).
2. Tay, T. L., Savage, J., Hui, C. W., Bisht, K., Tremblay, M.-È. Microglia across the lifespan: from origin to function in brain development, plasticity and cognition. *The Journal of Physiology* doi:10.1113/JP272134 (2016).
3. Davalos, D. *et al.* ATP mediates rapid microglial response to local brain injury *in vivo*. *Nature Neuroscience*. **8** (6), 752-758, doi:10.1038/nn1472 (2005).
4. Nimmerjahn, A. Resting Microglial Cells Are Highly Dynamic Surveillants of Brain Parenchyma in Vivo. *Science*. **308** (5726), 1314-1318, doi:10.1126/science.1110647 (2005).
5. Dissing-Olesen, L. *et al.* Activation of neuronal NMDA receptors triggers transient ATP-mediated microglial process outgrowth. *The Journal of Neuroscience: The Official Journal of the Society for Neuroscience*. **34** (32), 10511-10527, doi:10.1523/JNEUROSCI.0405-14.2014 (2014).
6. Gyoneva, S., Traynelis, S. F. Norepinephrine modulates the motility of resting and activated microglia *via* different adrenergic receptors. *Journal of Biological Chemistry*. **288** (21), 15291-15302, doi:10.1074/jbc.M113.458901 (2013).
7. Eyo, U. B. *et al.* Neuronal hyperactivity recruits microglial processes *via* neuronal NMDA receptors and microglial P2Y12 receptors after status epilepticus. *The Journal of Neuroscience: The Official Journal of the Society for Neuroscience*. **34** (32), 10528-10540, doi:10.1523/JNEUROSCI.0416-14.2014 (2014).

8. Hristovska, I., Pascual, O. Deciphering Resting Microglial Morphology and Process Motility from a Synaptic Prospect. *Frontiers in Integrative Neuroscience*. **9**, 1231, doi:10.1152/jn.01210.2007 (2016).
9. Avignone, E., Lepleux, M., Angibaud, J., Nägerl, U. V. Altered morphological dynamics of activated microglia after induction of status epilepticus. *Journal of Neuroinflammation*. **12**, 202, doi:10.1186/s12974-015-0421-6 (2015).
10. Abiega, O. *et al.* Neuronal Hyperactivity Disturbs ATP Microgradients, Impairs Microglial Motility, and Reduces Phagocytic Receptor Expression Triggering Apoptosis/Microglial Phagocytosis Uncoupling. *PLoS Biology*. **14** (5), e1002466, doi:10.1371/journal.pbio.1002466 (2016).
11. Madry, C. *et al.* Microglial Ramification, Surveillance, and Interleukin-1 β Release Are Regulated by the Two-Pore Domain K⁺Channel THIK-1. *Neuron*. **97** (2), 299-312.e6, doi:10.1016/j.neuron.2017.12.002 (2018).
12. Honda, S. *et al.* Extracellular ATP or ADP induce chemotaxis of cultured microglia through Gi/o-coupled P2Y receptors. *The Journal of Neuroscience: The Official Journal of the Society for Neuroscience*. **21** (6), 1975-1982 (2001).
13. Haynes, S. E. *et al.* The P2Y₁₂ receptor regulates microglial activation by extracellular nucleotides. *Nature Neuroscience*. **9** (12), 1512-1519, doi:10.1038/nn1805 (2006).
14. Wu, L.-J., Vadakkan, K. I., Zhuo, M. ATP-induced chemotaxis of microglial processes requires P2Y receptor-activated initiation of outward potassium currents. *Glia*. **55** (8), 810-821, doi:10.1002/glia.20500 (2007).
15. Kolodziejczak, M. *et al.* Serotonin Modulates Developmental Microglia via 5-HT 2B Receptors: Potential Implication during Synaptic Refinement of Retinogeniculate Projections. *ACS Chemical Neuroscience*. **6** (7), 1219-1230, doi:10.1021/cn5003489 (2015).
16. Schafer, D. P. *et al.* Microglia Sculpt Postnatal Neural Circuits in an Activity and Complement-Dependent Manner. *Neuron*. **74** (4), 691-705, doi:10.1016/j.neuron.2012.03.026 (2012).
17. Pfeiffer, T., Avignone, E., Nägerl, U. V. Induction of hippocampal long-term potentiation increases the morphological dynamics of microglial processes and prolongs their contacts with dendritic spines. *Scientific Reports*. **6**, 32422, doi:10.1038/srep32422 (2016).
18. Parkhurst, C. N. *et al.* Microglia Promote Learning-Dependent Synapse Formation through Brain-Derived Neurotrophic Factor. *Cell*. **155** (7), 1596-1609, doi:10.1016/j.cell.2013.11.030 (2013).

19. Wu, Y., Dissing-Olesen, L., Macvicar, B. A., Stevens, B. Microglia: Dynamic Mediators of Synapse Development and Plasticity. *Trends in Immunology*. **36** (10), 605-613, doi:10.1016/j.it.2015.08.008 (2015).
20. Ohsawa, K. *et al.* P2Y₁₂ receptor-mediated integrin-beta1 activation regulates microglial process extension induced by ATP. *Glia*. **58** (7), 790-801, doi:10.1002/glia.20963 (2010).
21. Kurpius, D., Wilson, N., Fuller, L., Hoffman, A., Dailey, M. E. Early activation, motility, and homing of neonatal microglia to injured neurons does not require protein synthesis. *Glia*. **54** (1), 58-70, doi:10.1002/glia.20355 (2006).
22. Stence, N., Waite, M., Dailey, M. E. Dynamics of microglial activation: a confocal time-lapse analysis in hippocampal slices. *Glia*. **33** (3), 256-266 (2001).
23. Dissing-Olesen, L., Macvicar, B. A. Fixation and Immunolabeling of Brain Slices: SNAPSHOT Method. *Current Protocols in Neuroscience*. **71**, 1.23.1-12, doi:10.1002/0471142301.ns0123s71 (2015).
24. Schindelin, J. *et al.* Fiji: an open-source platform for biological-image analysis. *Nature Methods*. **9** (7), 676-682, doi:10.1038/nmeth.2019 (2012).
25. de Chaumont, F. *et al.* Icy: an open bioimage informatics platform for extended reproducible research. *Nature Methods*. **9** (7), 690-696, doi:10.1038/nmeth.2075 (2012).
26. Aitken, P. G. *et al.* Preparative methods for brain slices: a discussion. *Journal of Neuroscience Methods*. **59** (1), 139-149 (1995).
27. Paris, I. *et al.* ProMolJ: A new tool for automatic three-dimensional analysis of microglial process motility. *Glia*. **66** (4), 828-845, doi:10.1002/glia.23287 (2018).
28. Pagani, F. *et al.* Defective microglial development in the hippocampus of Cx3cr1 deficient mice. *Frontiers in Cellular Neuroscience*. **9** (229), 111, doi:10.3389/fncel.2015.00111 (2015).
29. Ting, J. T., Daigle, T. L., Chen, Q., Feng, G. Acute brain slice methods for adult and aging animals: application of targeted patch clamp analysis and optogenetics. *Methods in Molecular Biology* (Clifton, NJ). **1183**, 221-242, doi:10.1007/978-1-4939-1096-0_14 (2014).
30. Mainen, Z. F. *et al.* Two-photon imaging in living brain slices. *Methods* (San Diego, CA). **18** (2), 231-239, 181, doi:10.1006/meth.1999.0776 (1999).
31. Tanaka, Y., Tanaka, Y., Furuta, T., Yanagawa, Y., Kaneko, T. The effects of cutting solutions on the viability of GABAergic interneurons in cerebral cortical slices of adult mice. *Journal of Neuroscience Methods*. **171** (1), 118-125, doi:10.1016/j.jneumeth.2008.02.021 (2008).

- 918 32. Gyoneva, S. *et al.* Systemic inflammation regulates microglial responses to tissue damage *in*
919 *vivo*. *Glia*. **62** (8), 1345-1360, doi:10.1002/glia.22686 (2014).
920
- 921 33. Heindl, S. *et al.* Automated Morphological Analysis of Microglia After Stroke. *Frontiers in*
922 *Cellular Neuroscience*. **12**, 106, doi:10.3389/fncel.2018.00106 (2018).
923
- 924 34. Dailey, M. E., Eyo, U., Fuller, L., Hass, J., Kurpius, D. Imaging microglia in brain slices and slice
925 cultures. *Cold Spring Harbor Protocols*. **2013** (12), 1142-1148, doi:10.1101/pdb.prot079483
926 (2013).
927

Figure 1

[Click here to access/download;Figure;Etienne_Figure1.eps](#)

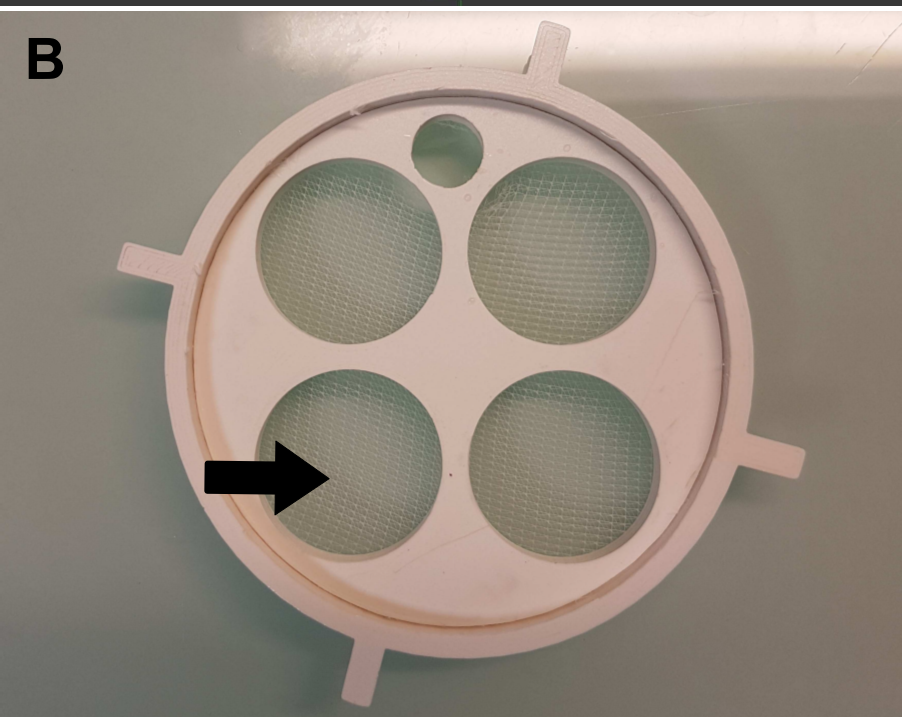
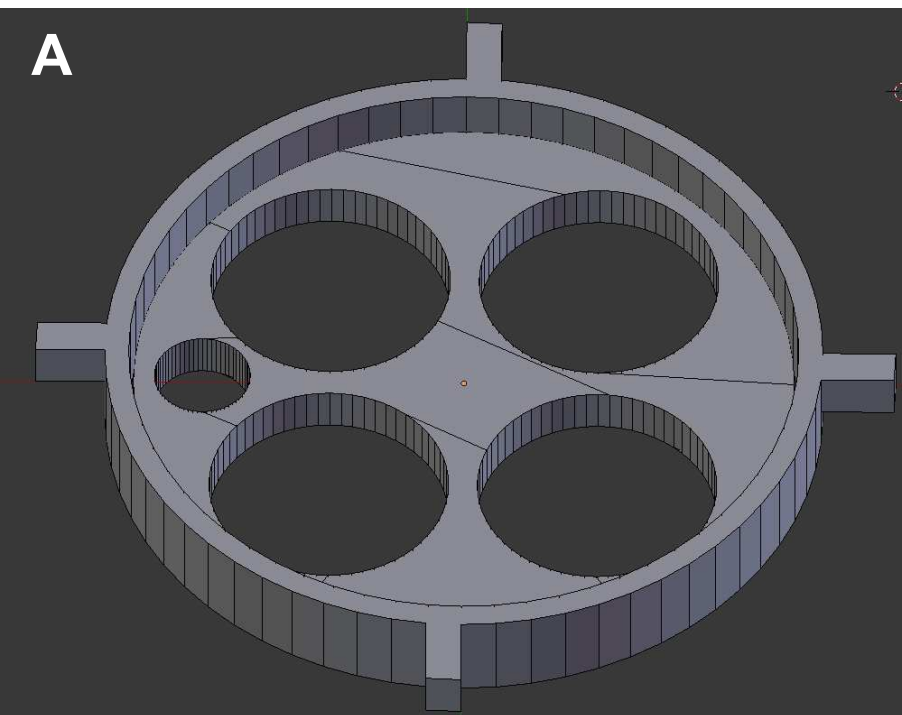


Figure 2

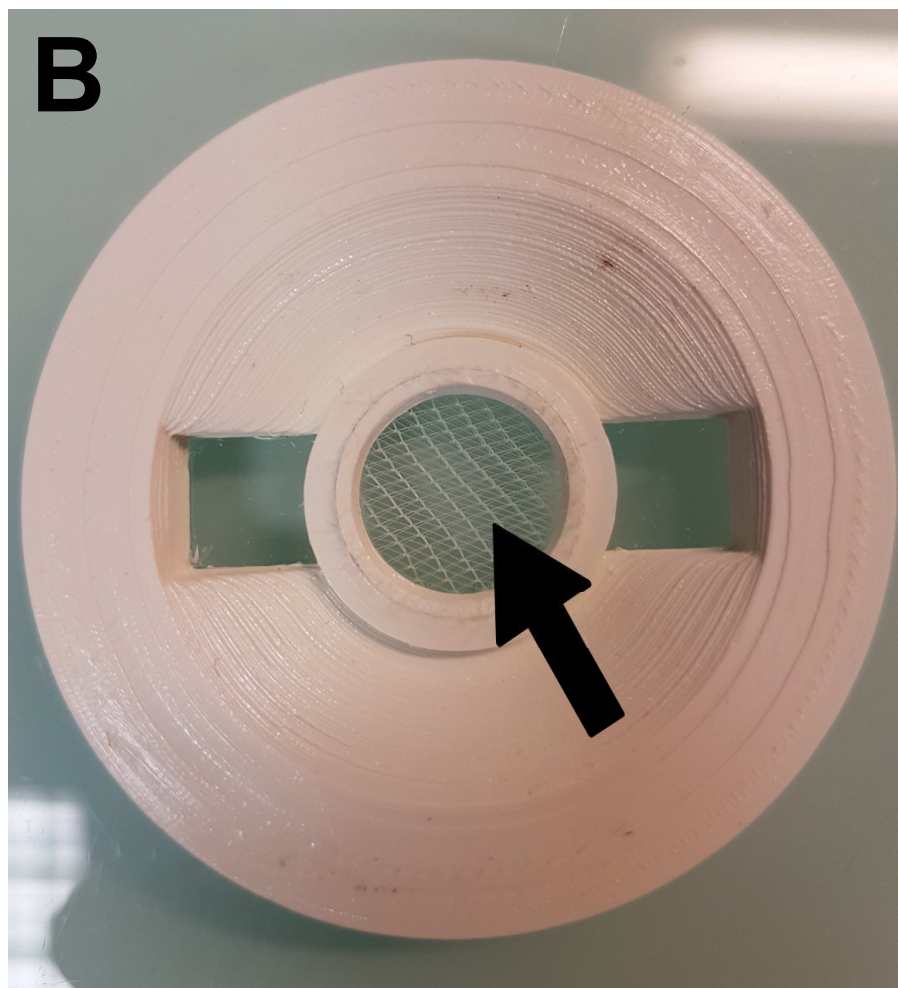
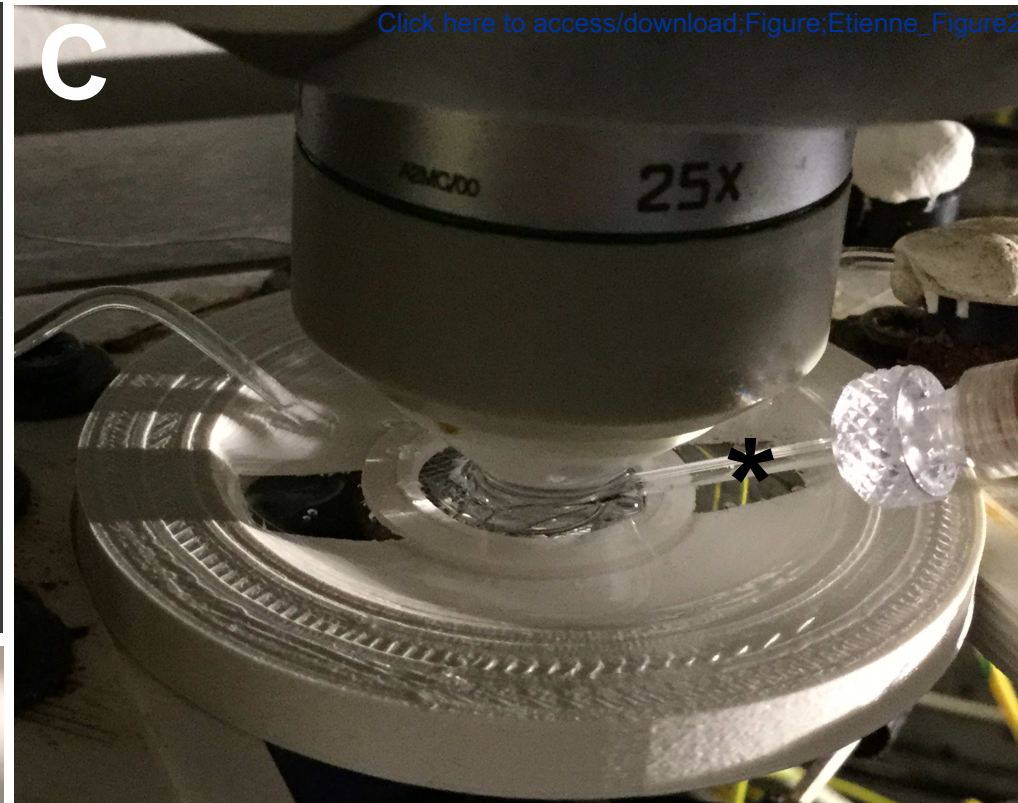
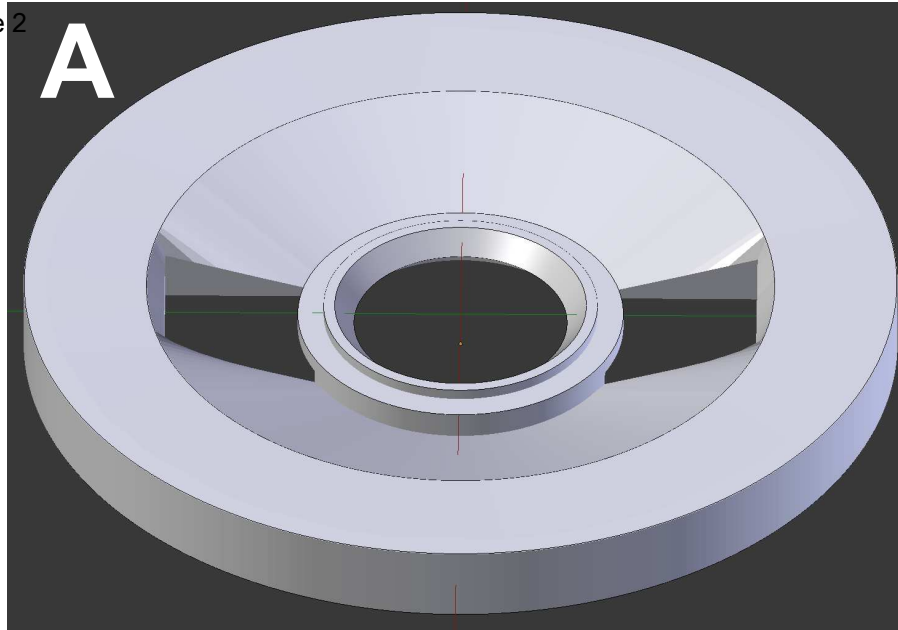
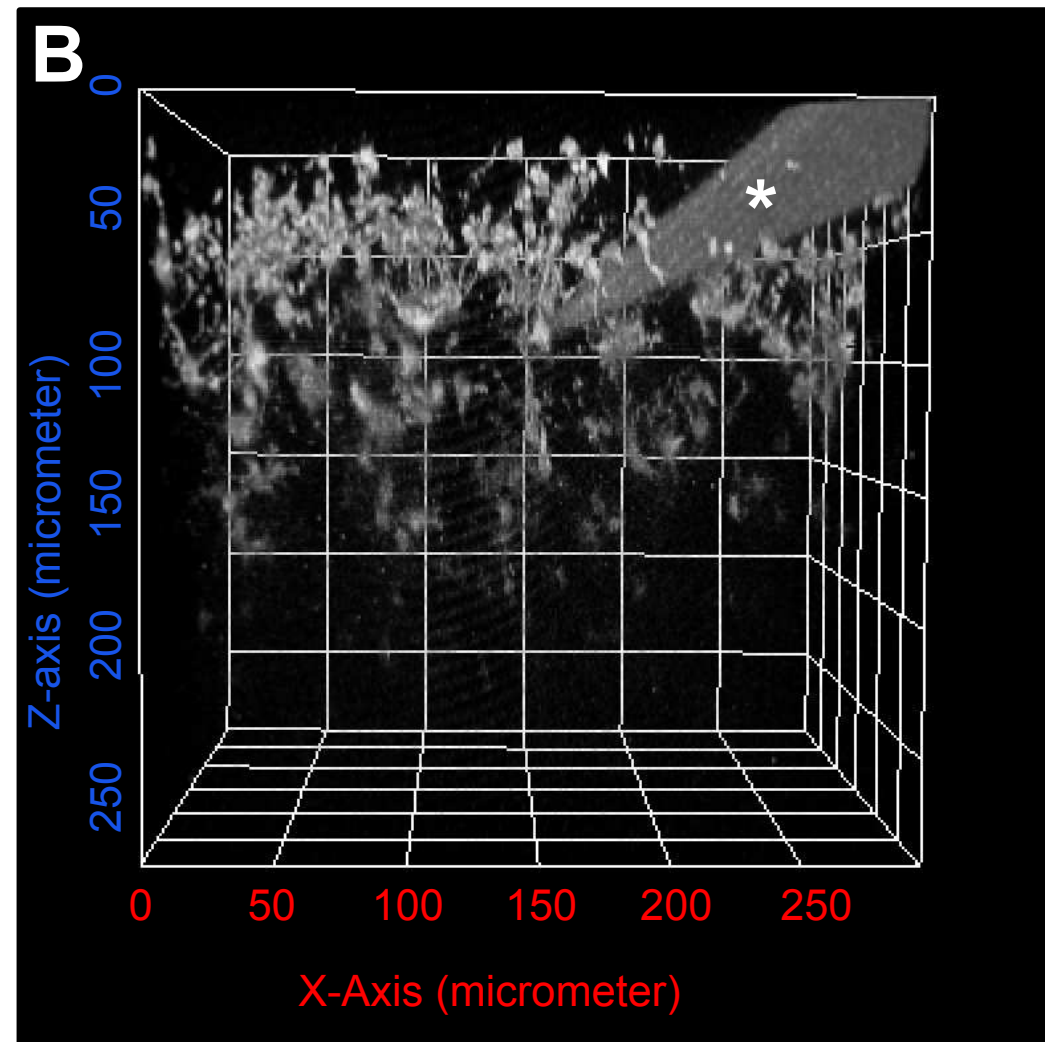
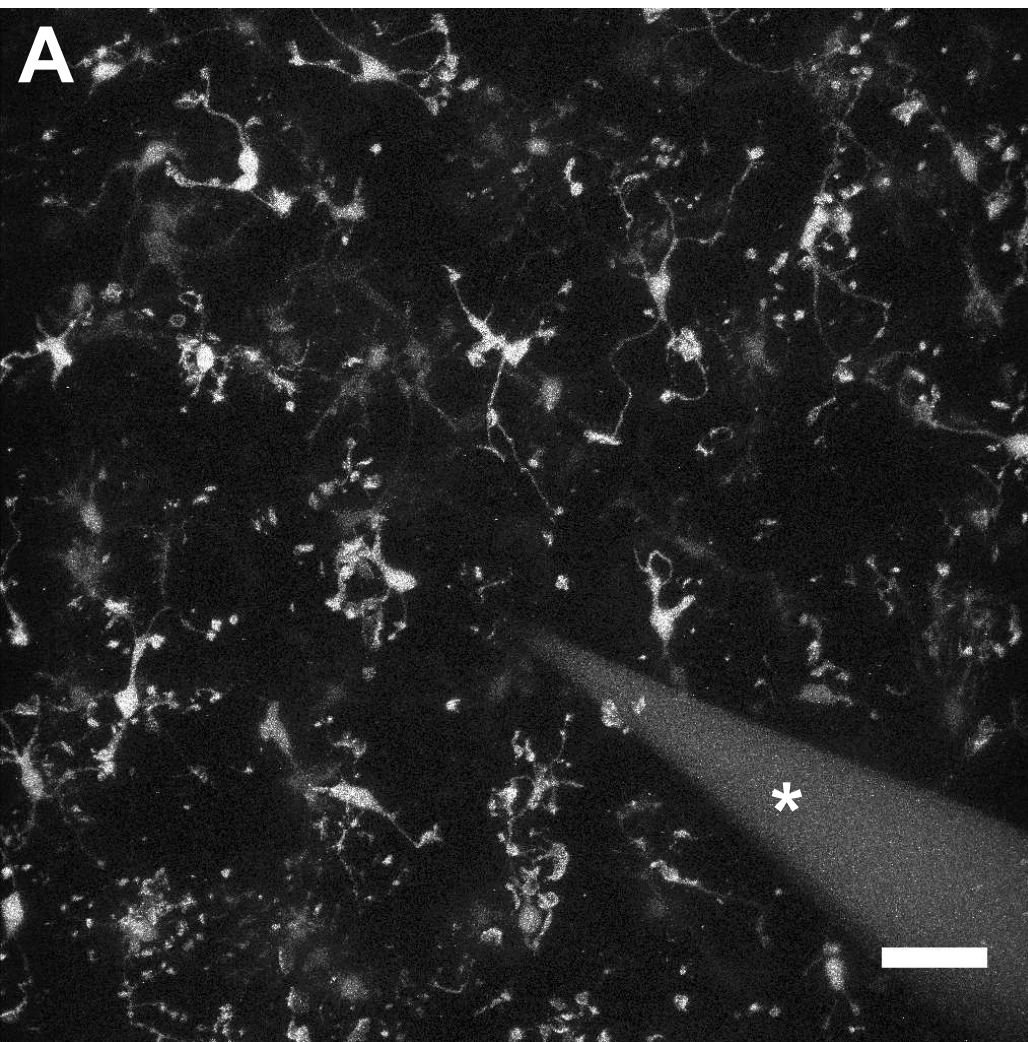
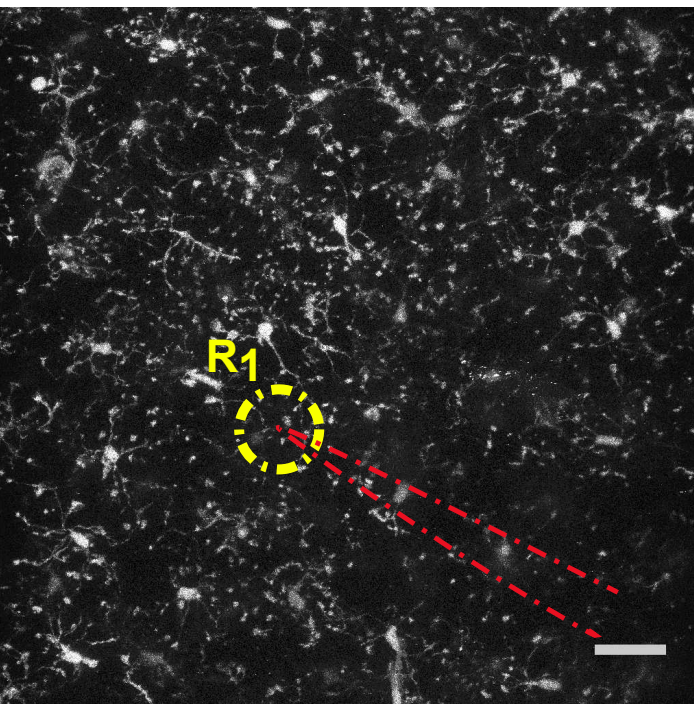


Figure 3

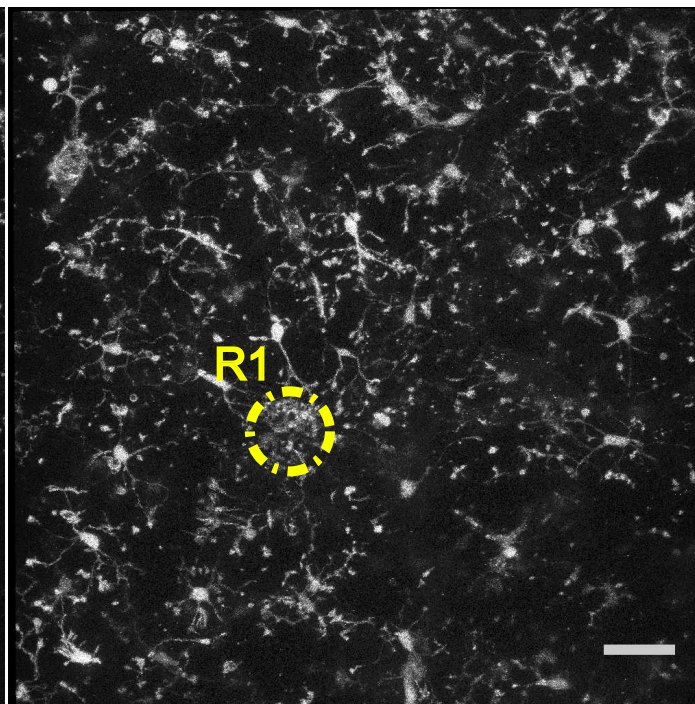
[Click here to access/download;Figure;Etienne_Figure3.eps](#) 



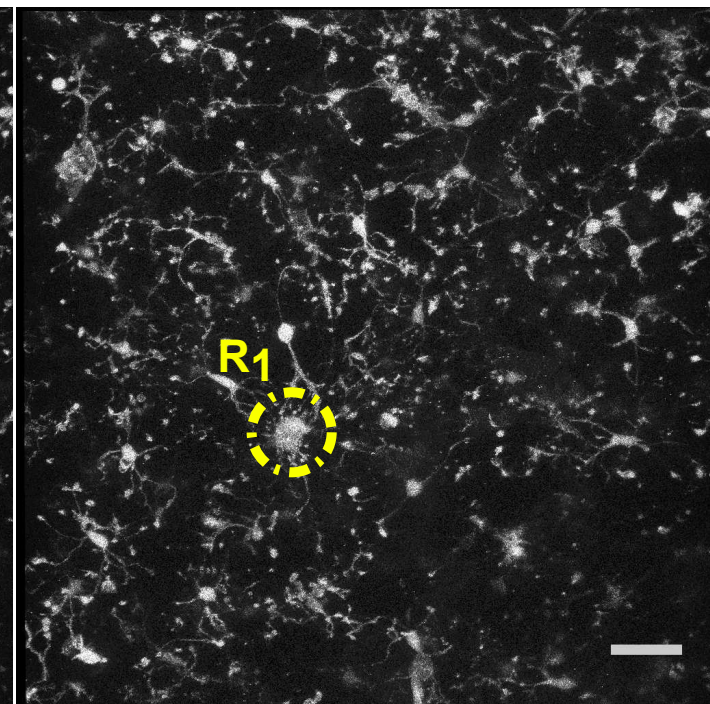
Before injection



10 min after injection



25 min after injection

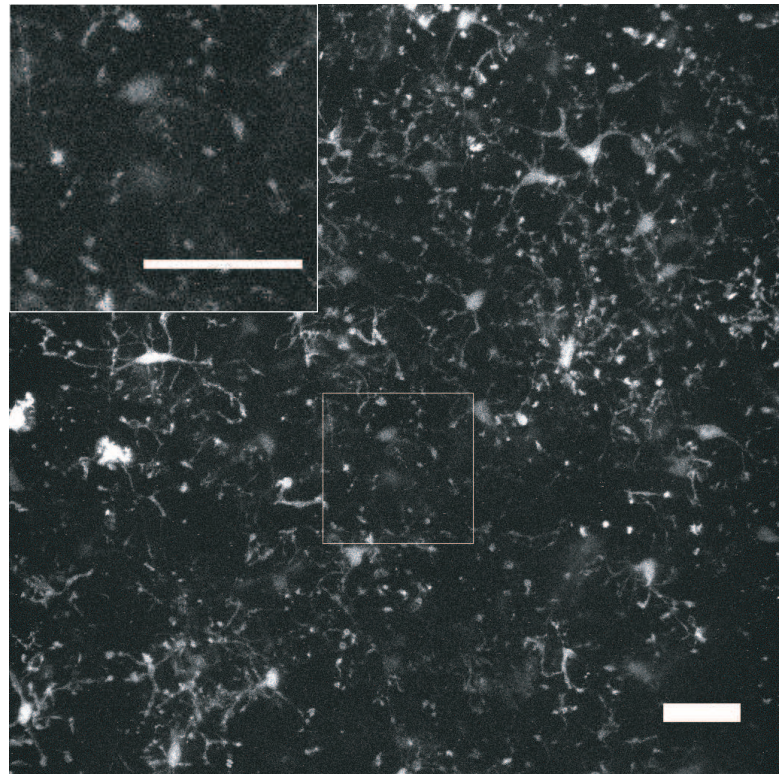
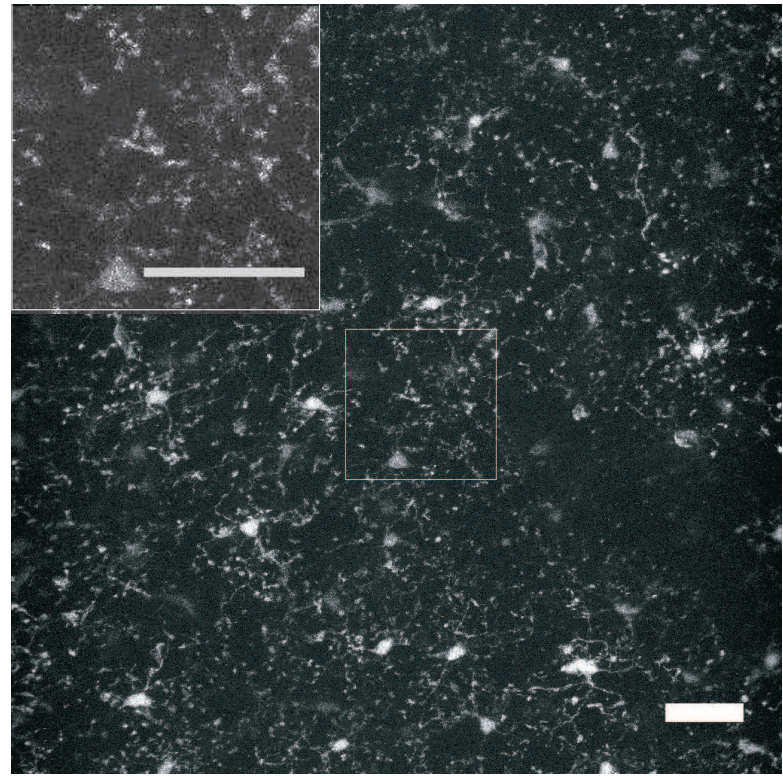


5-HT - 20 days old

ATP 2 months old

[Click here to download Figure;Etienne_Figure5.eps](#)

Before injection



After injection

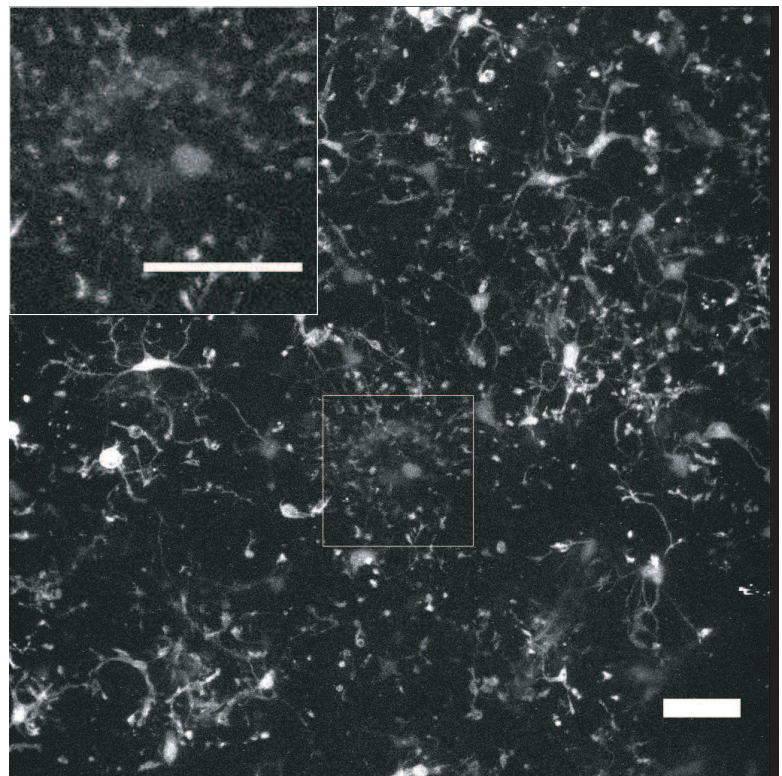
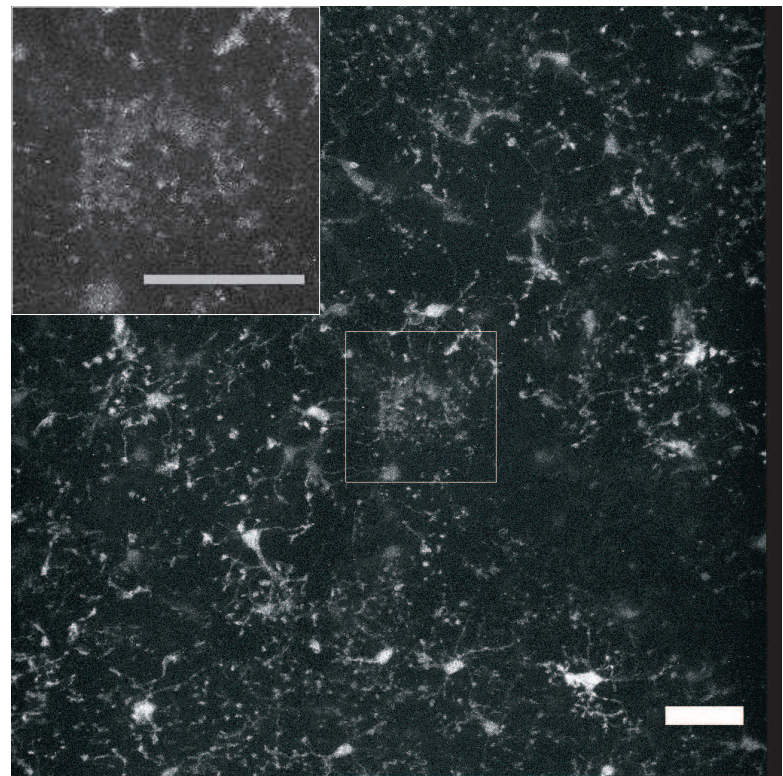


Figure 6

[Click here to access/download;Figure;Etienne_Figure6.eps](#) 

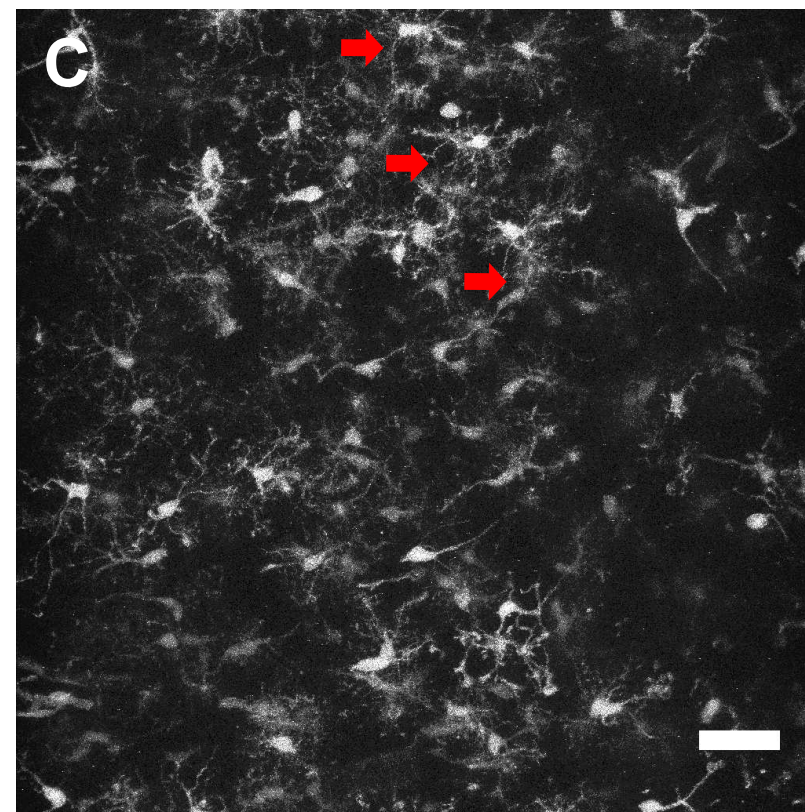
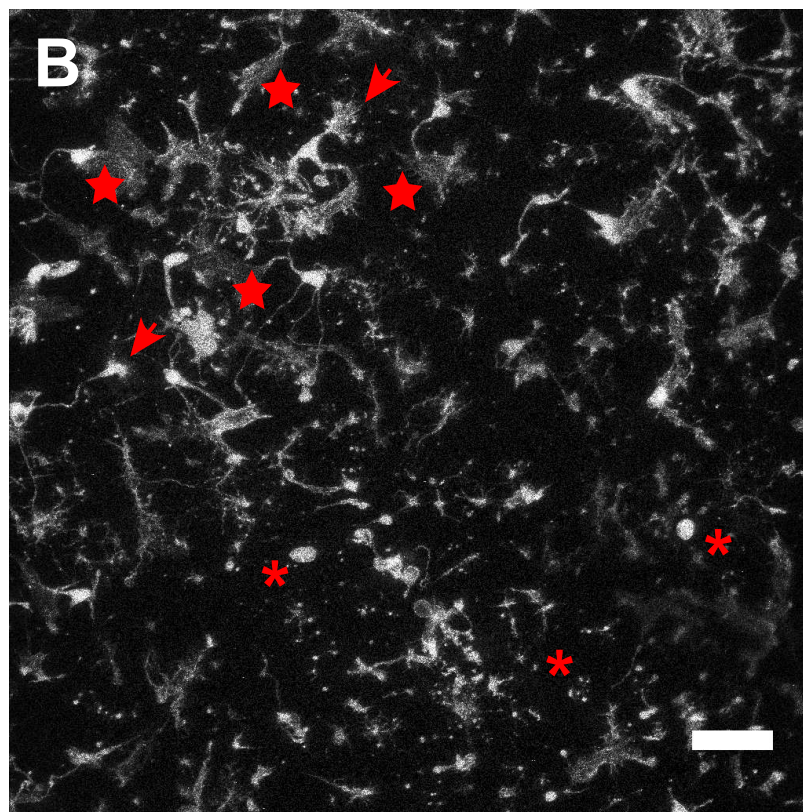
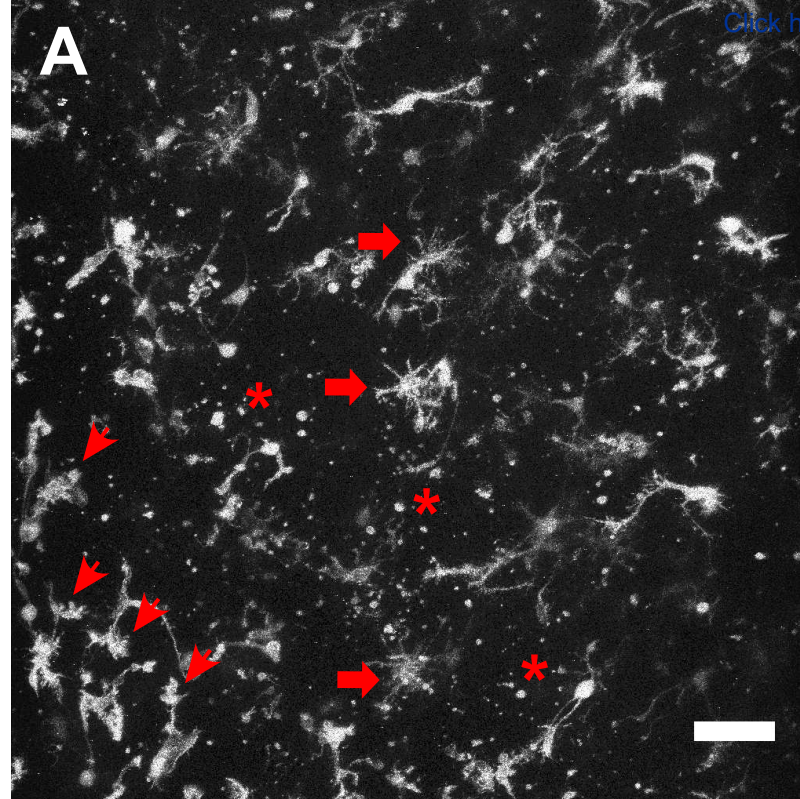
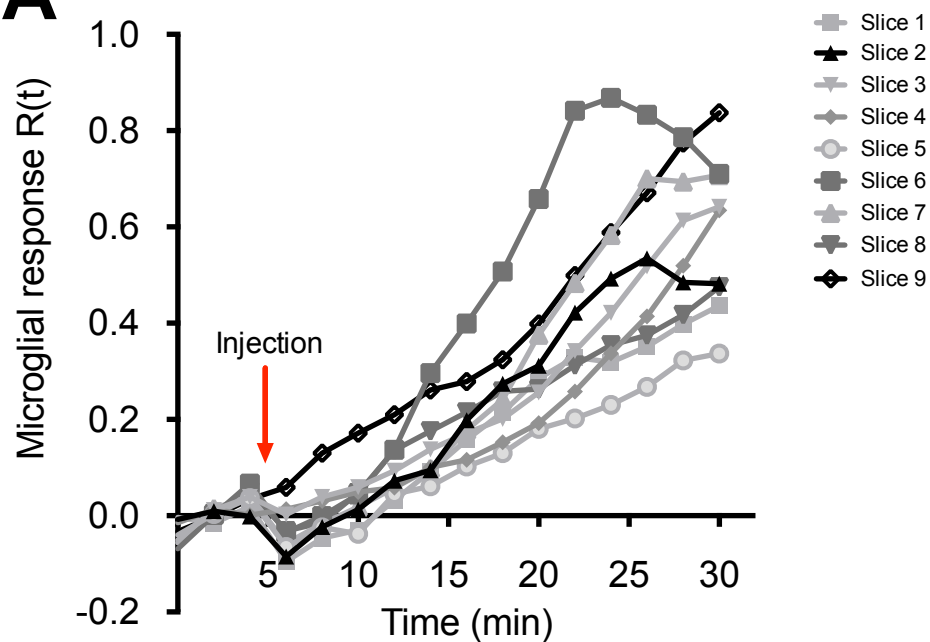
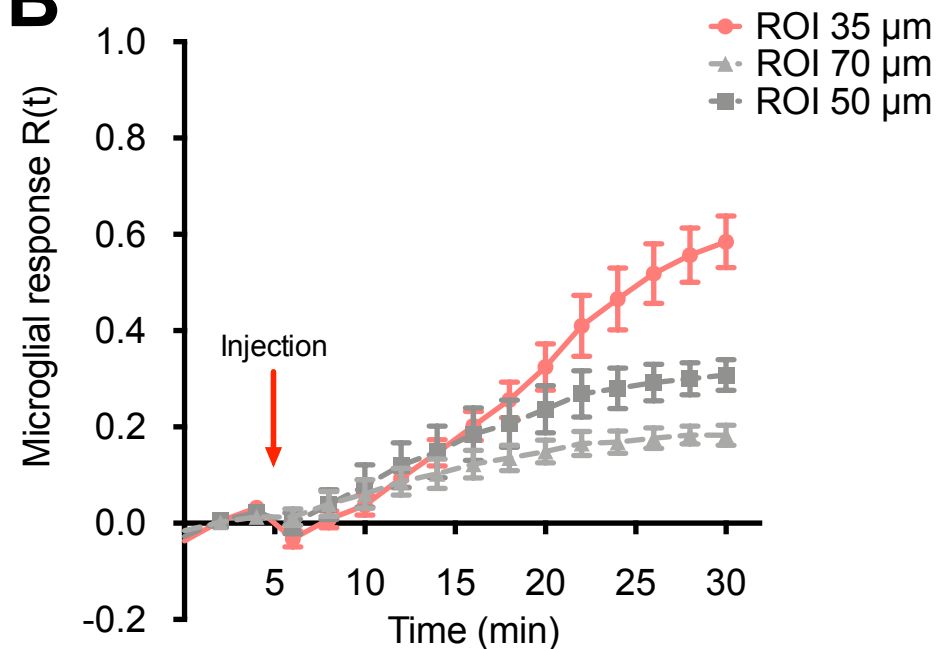
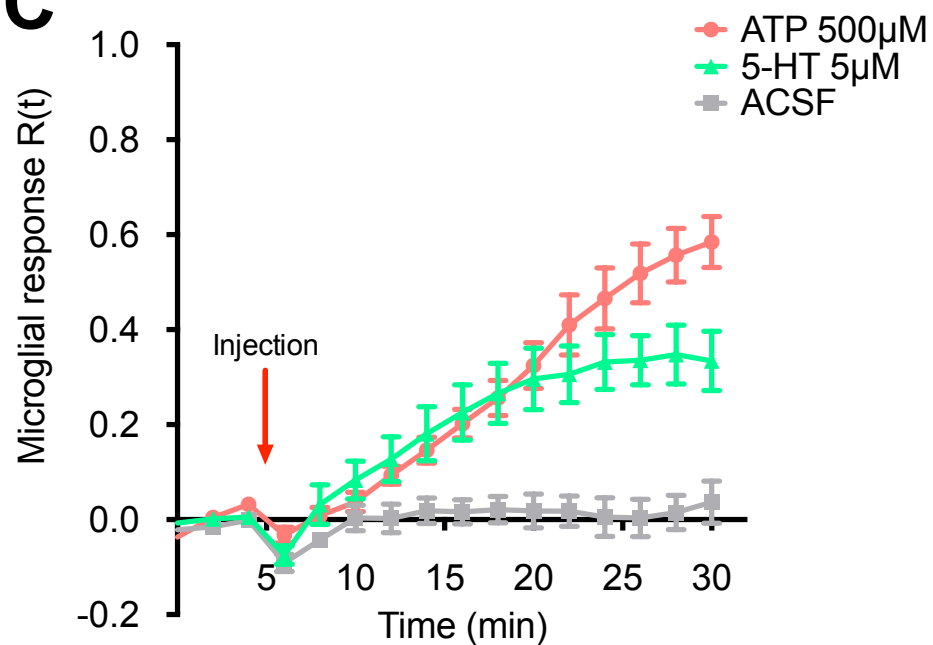
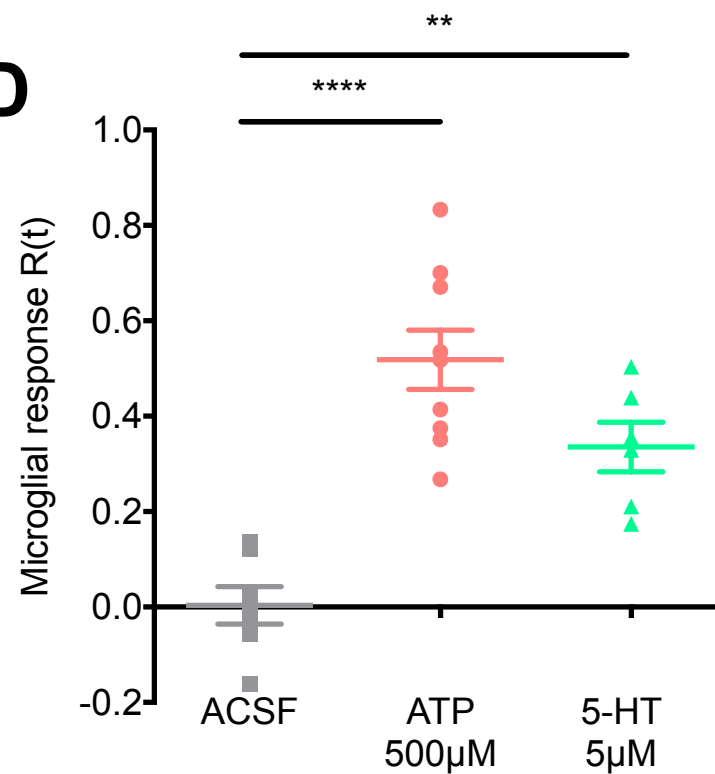
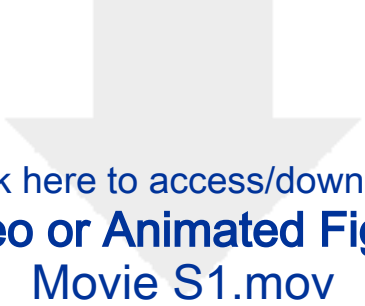
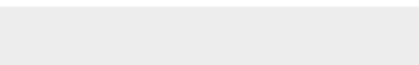




Figure 7

A**B****C****D**

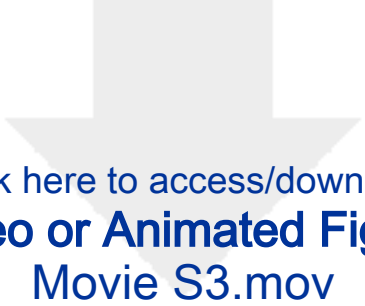


Click here to access/download
Video or Animated Figure
Movie S1.mov

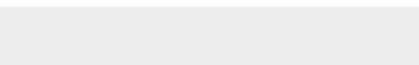



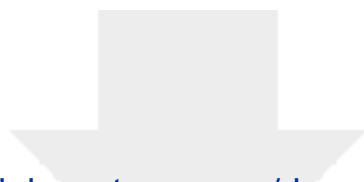


Click here to access/download
Video or Animated Figure
Movie S2.mov



Click here to access/download
Video or Animated Figure
Movie S3.mov

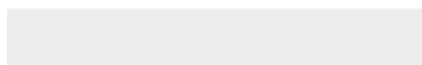
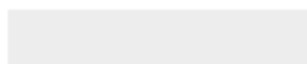




[Click here to access/download](#)

Video or Animated Figure

MAX_110118_ATP_creYFP (converti).mov



Name of Material/ Equipment	Company
for pipettes preparation	
Clark Borosilicate Thin Wall Capillaries	Harvard Apparatus
DMZ Universal Puller	Zeitz Instrumente
for solutions	
Calcium Chloride dihydrate (CaCl ₂)	Sigma
Choline Chloride	Sigma
D-(+)-Glucose	Sigma
L-Ascorbic acid	Sigma
Magnesium Chloride solution 1M (MgCl ₂)	Sigma
Potassium chloride SigmaUltra >99,0% (KCl)	Sigma
Sodium bicarbonate (NaHCO ₃)	Sigma
Sodium Chloride (NaCl)	Sigma
Sodium phosphate monobasic	Sigma
Sodium pyruvate	Sigma
Ultrapure water	MilliQ
for slice preparation	
2x 200 mL crystalizing dishes	
80 mL Pyrex beaker	
Antlia-3C Digital Peristaltic pump	DD Biolab

Carbogen 5% CO ₂ /95% O ₂	Air Liquide France
Dolethal	Industrie Vetoquinol
Filter papers (Whatman)	Sigma
Fine Scissors - Sharp	Fine Science Tools
Food box 10 cm diameter, 8 cm Height	
glue (ethyl cyanoacrylate)	Loctite
Hippocampal Tool (spatula)	Fine Science Tools
Ice	
Iris Forceps (curved)	Moria
Lens cleaning tissue	THOR LABS
Nylon mesh strainer	
Razor blades	Electron Microscopy Sciences
scalpel blade	
Slice interface holder	
Surgical Scissors - Sharp	Fine Science Tools
Vibrating slicer	Thermo Scientific
Water bath	
for slice imaging	
× 25 0.95 NA water-immersion objective	Leica Microsystems (Germany)
2-photon MP5 upright microscope with resonant scanners (8 kHz) and two HyD Hybrid detectors	Leica Microsystems (Germany)

Antlia-3C Digital Peristaltic pump	DD Biolab
Carbogen 5% CO ₂ /95% O ₂	Air Liquide France Industrie
Chameleon Ultra2 Ti:sapphire laser	Coherent (Germany)
disposable transfer pipettes , wide mouth	ThermoFischer scientific
emission filter SP680	Leica Microsystems (Germany)
fluorescent cube containing a 525/50 emission filter and a 560 dichroic filter (for fluorescence collection)	Leica Microsystems (Germany)
glass beaker with 50 mL of ACSF to maintain constant perfusion of the slice	
Heating system	Warner Instrument Corporation
perfusion chamber	
slice holder ("harp")	

for slice stimulation

Adenosine 5'-triphosphate disodium salt hydrate (ATP)	Sigma
--	-------

Fluorescein (optional)

Micromanipulator

Micropipette holder

Sigma
Luigs and
Neumann

Serotonin hydrochloride

Sigma

Syringe 5mL (without needle)

Terumo medical
products

Transparent tubing

Fischer Scientific

for image analysis

Fiji

Icy

Institut Pasteur

mice

CX3CR1-GFP mice

Jung et al, 2000

CX3CR1creER-YFP mice

Parkhurst et al
2013

Catalog Number	Comments/Description
30-0065	Borosilicate Thin Wall without Filament, 1.5 mm
C5080	
C7527	
G8270	
A5960	
63020	
P9333	
S5761	
S5886	
S5011	
P2256	
	for all the solutions
178961	For mice perfusion and 2- photon chamber

Dolethal 50 mg/mL

WHA1001042

14060-60

Whatman qualitative filter
paper, Grade 1 (Pore size:
11 μ M)

super glue 3 power flex

10099-15

MC31

The largest extremity has
to be angled at 90 °

diameter 7 cm

72000

For the slicer

home-made, the file for
3D printing is provided in
Supplemental Material

14002-14

720-2709

Model: HM 650V
(Vibrating blade
microtome)
Set at 32°C (first recovery
step)

HCX Irapo

178961

For 2-photon chamber
perfusion with aCSF

I1501L50R2A001

for example : 232-11

5.8ml with fin tip, but we
cut it (approx 7cm) to
have a 4 mm diameter
mouth

Automatic Heater Controller TC-324B

to maintain perfusion
solution at 32°C

home-made, the file for
3D printing is provided in
Supplemental Material

home made : hairpin
made of platinum with
the two branches joined
by parallel nylon threads

A-26209

to be prepared ex-
temporaneously : 1mg/ml
(3mM) stock solution
prepared the day of the
experiment, kept at 4°C
(a few hours) and diluted
just before use

F-6377

SM7

use at 1 μ M final
connected to the
micropipette holde
same as for
eletrophysiology
aliquots of 50mM stock
solution in H2O kept at -
20°C. 500 μ M solution
prepared the day of the
experiment.

H-9523

SS+05S1

11750105

Saint Gobain Performance
Plastics™ Tygon™ E-3603
Non-DEHP Tubing

<https://fiji.sc>

Schindelin, J. et al Nat.
Methods (2012) doi
10.1038

<http://icy.bioimageanalysis.org>

de Chaumont, F. et al.
Nat. Methods (2012)

male or females, P3 to 2
months-old ; we have
backcrossed these mice
on 129sv background.
male or females, P3 to 2
months-old ; we have
backcrossed these mice
on 129sv background.



1 Alewife Center #200
Cambridge, MA 02140
tel. 617.945.9051
www.jove.com

ARTICLE AND VIDEO LICENSE AGREEMENT

Title of Article:	2-photon imaging of microglial processes attraction toward ATP or serotonin in acute brain slices of young and adult mice
Author(s):	Etienne, F, Mastrolia, V, Maroteaux, L, Girault JA, Gervasi, N* , Roumier, A* (*equal contribution)

Item 1: The Author elects to have the Materials be made available (as described at <http://www.jove.com/publish>) via:



Standard Access



Open Access

Item 2: Please select one of the following items:



The Author is **NOT** a United States government employee.



The Author is a United States government employee and the Materials were prepared in the course of his or her duties as a United States government employee.



The Author is a United States government employee but the Materials were NOT prepared in the course of his or her duties as a United States government employee.

ARTICLE AND VIDEO LICENSE AGREEMENT

1. **Defined Terms.** As used in this Article and Video License Agreement, the following terms shall have the following meanings: **"Agreement"** means this Article and Video License Agreement; **"Article"** means the article specified on the last page of this Agreement, including any associated materials such as texts, figures, tables, artwork, abstracts, or summaries contained therein; **"Author"** means the author who is a signatory to this Agreement; **"Collective Work"** means a work, such as a periodical issue, anthology or encyclopedia, in which the Materials in their entirety in unmodified form, along with a number of other contributions, constituting separate and independent works in themselves, are assembled into a collective whole; **"CRC License"** means the Creative Commons Attribution-Non Commercial-No Derivs 3.0 Unported Agreement, the terms and conditions of which can be found at: <http://creativecommons.org/licenses/by-nc-nd/3.0/legalcode>; **"Derivative Work"** means a work based upon the Materials or upon the Materials and other pre-existing works, such as a translation, musical arrangement, dramatization, fictionalization, motion picture version, sound recording, art reproduction, abridgment, condensation, or any other form in which the Materials may be recast, transformed, or adapted; **"Institution"** means the institution, listed on the last page of this Agreement, by which the Author was employed at the time of the creation of the Materials; **"JoVE"** means MyJoVE Corporation, a Massachusetts corporation and the publisher of The Journal of Visualized Experiments; **"Materials"** means the Article and / or the Video; **"Parties"** means the Author and JoVE; **"Video"** means any video(s) made by the Author, alone or in conjunction with any other parties, or by JoVE or its affiliates or agents, individually or in collaboration with the Author or any other parties, incorporating all or any portion

of the Article, and in which the Author may or may not appear.

2. **Background.** The Author, who is the author of the Article, in order to ensure the dissemination and protection of the Article, desires to have the JoVE publish the Article and create and transmit videos based on the Article. In furtherance of such goals, the Parties desire to memorialize in this Agreement the respective rights of each Party in and to the Article and the Video.

3. **Grant of Rights in Article.** In consideration of JoVE agreeing to publish the Article, the Author hereby grants to JoVE, subject to **Sections 4** and **7** below, the exclusive, royalty-free, perpetual (for the full term of copyright in the Article, including any extensions thereto) license (a) to publish, reproduce, distribute, display and store the Article in all forms, formats and media whether now known or hereafter developed (including without limitation in print, digital and electronic form) throughout the world, (b) to translate the Article into other languages, create adaptations, summaries or extracts of the Article or other Derivative Works (including, without limitation, the Video) or Collective Works based on all or any portion of the Article and exercise all of the rights set forth in (a) above in such translations, adaptations, summaries, extracts, Derivative Works or Collective Works and (c) to license others to do any or all of the above. The foregoing rights may be exercised in all media and formats, whether now known or hereafter devised, and include the right to make such modifications as are technically necessary to exercise the rights in other media and formats. If the "Open Access" box has been checked in **Item 1** above, JoVE and the Author hereby grant to the public all such rights in the Article as provided in, but subject to all limitations and requirements set forth in, the CRC License.

ARTICLE AND VIDEO LICENSE AGREEMENT

4. **Retention of Rights in Article.** Notwithstanding the exclusive license granted to JoVE in **Section 3** above, the Author shall, with respect to the Article, retain the non-exclusive right to use all or part of the Article for the non-commercial purpose of giving lectures, presentations or teaching classes, and to post a copy of the Article on the Institution's website or the Author's personal website, in each case provided that a link to the Article on the JoVE website is provided and notice of JoVE's copyright in the Article is included. All non-copyright intellectual property rights in and to the Article, such as patent rights, shall remain with the Author.

5. **Grant of Rights in Video – Standard Access.** This **Section 5** applies if the "Standard Access" box has been checked in **Item 1** above or if no box has been checked in **Item 1** above. In consideration of JoVE agreeing to produce, display or otherwise assist with the Video, the Author hereby acknowledges and agrees that, Subject to **Section 7** below, JoVE is and shall be the sole and exclusive owner of all rights of any nature, including, without limitation, all copyrights, in and to the Video. To the extent that, by law, the Author is deemed, now or at any time in the future, to have any rights of any nature in or to the Video, the Author hereby disclaims all such rights and transfers all such rights to JoVE.

6. **Grant of Rights in Video – Open Access.** This **Section 6** applies only if the "Open Access" box has been checked in **Item 1** above. In consideration of JoVE agreeing to produce, display or otherwise assist with the Video, the Author hereby grants to JoVE, subject to **Section 7** below, the exclusive, royalty-free, perpetual (for the full term of copyright in the Article, including any extensions thereto) license (a) to publish, reproduce, distribute, display and store the Video in all forms, formats and media whether now known or hereafter developed (including without limitation in print, digital and electronic form) throughout the world, (b) to translate the Video into other languages, create adaptations, summaries or extracts of the Video or other Derivative Works or Collective Works based on all or any portion of the Video and exercise all of the rights set forth in (a) above in such translations, adaptations, summaries, extracts, Derivative Works or Collective Works and (c) to license others to do any or all of the above. The foregoing rights may be exercised in all media and formats, whether now known or hereafter devised, and include the right to make such modifications as are technically necessary to exercise the rights in other media and formats. For any Video to which this **Section 6** is applicable, JoVE and the Author hereby grant to the public all such rights in the Video as provided in, but subject to all limitations and requirements set forth in, the CRC License.

7. **Government Employees.** If the Author is a United States government employee and the Article was prepared in the course of his or her duties as a United States government employee, as indicated in **Item 2** above, and any of the licenses or grants granted by the Author hereunder exceed the scope of the 17 U.S.C. 403, then the rights granted hereunder shall be limited to the maximum

rights permitted under such statute. In such case, all provisions contained herein that are not in conflict with such statute shall remain in full force and effect, and all provisions contained herein that do so conflict shall be deemed to be amended so as to provide to JoVE the maximum rights permissible within such statute.

8. **Protection of the Work.** The Author(s) authorize JoVE to take steps in the Author(s) name and on their behalf if JoVE believes some third party could be infringing or might infringe the copyright of either the Author's Article and/or Video.

9. **Likeness, Privacy, Personality.** The Author hereby grants JoVE the right to use the Author's name, voice, likeness, picture, photograph, image, biography and performance in any way, commercial or otherwise, in connection with the Materials and the sale, promotion and distribution thereof. The Author hereby waives any and all rights he or she may have, relating to his or her appearance in the Video or otherwise relating to the Materials, under all applicable privacy, likeness, personality or similar laws.

10. **Author Warranties.** The Author represents and warrants that the Article is original, that it has not been published, that the copyright interest is owned by the Author (or, if more than one author is listed at the beginning of this Agreement, by such authors collectively) and has not been assigned, licensed, or otherwise transferred to any other party. The Author represents and warrants that the author(s) listed at the top of this Agreement are the only authors of the Materials. If more than one author is listed at the top of this Agreement and if any such author has not entered into a separate Article and Video License Agreement with JoVE relating to the Materials, the Author represents and warrants that the Author has been authorized by each of the other such authors to execute this Agreement on his or her behalf and to bind him or her with respect to the terms of this Agreement as if each of them had been a party hereto as an Author. The Author warrants that the use, reproduction, distribution, public or private performance or display, and/or modification of all or any portion of the Materials does not and will not violate, infringe and/or misappropriate the patent, trademark, intellectual property or other rights of any third party. The Author represents and warrants that it has and will continue to comply with all government, institutional and other regulations, including, without limitation all institutional, laboratory, hospital, ethical, human and animal treatment, privacy, and all other rules, regulations, laws, procedures or guidelines, applicable to the Materials, and that all research involving human and animal subjects has been approved by the Author's relevant institutional review board.

11. **JoVE Discretion.** If the Author requests the assistance of JoVE in producing the Video in the Author's facility, the Author shall ensure that the presence of JoVE employees, agents or independent contractors is in accordance with the relevant regulations of the Author's institution. If more than one author is listed at the beginning of this Agreement, JoVE may, in its sole

ARTICLE AND VIDEO LICENSE AGREEMENT

discretion, elect not take any action with respect to the Article until such time as it has received complete, executed Article and Video License Agreements from each such author. JoVE reserves the right, in its absolute and sole discretion and without giving any reason therefore, to accept or decline any work submitted to JoVE. JoVE and its employees, agents and independent contractors shall have full, unfettered access to the facilities of the Author or of the Author's institution as necessary to make the Video, whether actually published or not. JoVE has sole discretion as to the method of making and publishing the Materials, including, without limitation, to all decisions regarding editing, lighting, filming, timing of publication, if any, length, quality, content and the like.

12. **Indemnification.** The Author agrees to indemnify JoVE and/or its successors and assigns from and against any and all claims, costs, and expenses, including attorney's fees, arising out of any breach of any warranty or other representations contained herein. The Author further agrees to indemnify and hold harmless JoVE from and against any and all claims, costs, and expenses, including attorney's fees, resulting from the breach by the Author of any representation or warranty contained herein or from allegations or instances of violation of intellectual property rights, damage to the Author's or the Author's institution's facilities, fraud, libel, defamation, research, equipment, experiments, property damage, personal injury, violations of institutional, laboratory, hospital, ethical, human and animal treatment, privacy or other rules, regulations, laws, procedures or guidelines, liabilities and other losses or damages related in any way to the submission of work to JoVE, making of videos by JoVE, or publication in JoVE or elsewhere by JoVE. The Author shall be responsible for, and shall hold JoVE harmless from, damages caused by lack of sterilization, lack of cleanliness or by contamination due to

the making of a video by JoVE its employees, agents or independent contractors. All sterilization, cleanliness or decontamination procedures shall be solely the responsibility of the Author and shall be undertaken at the Author's expense. All indemnifications provided herein shall include JoVE's attorney's fees and costs related to said losses or damages. Such indemnification and holding harmless shall include such losses or damages incurred by, or in connection with, acts or omissions of JoVE, its employees, agents or independent contractors.

13. **Fees.** To cover the cost incurred for publication, JoVE must receive payment before production and publication the Materials. Payment is due in 21 days of invoice. Should the Materials not be published due to an editorial or production decision, these funds will be returned to the Author. Withdrawal by the Author of any submitted Materials after final peer review approval will result in a US\$1,200 fee to cover pre-production expenses incurred by JoVE. If payment is not received by the completion of filming, production and publication of the Materials will be suspended until payment is received.

14. **Transfer, Governing Law.** This Agreement may be assigned by JoVE and shall inure to the benefits of any of JoVE's successors and assignees. This Agreement shall be governed and construed by the internal laws of the Commonwealth of Massachusetts without giving effect to any conflict of law provision thereunder. This Agreement may be executed in counterparts, each of which shall be deemed an original, but all of which together shall be deemed to be one and the same agreement. A signed copy of this Agreement delivered by facsimile, e-mail or other means of electronic transmission shall be deemed to have the same legal effect as delivery of an original signed copy of this Agreement.

A signed copy of this document must be sent with all new submissions. Only one Agreement is required per submission.

CORRESPONDING AUTHOR

Name:

Anne Roumier

Department:

Institut du Fer à Moulin - Team 5

Institution:

Title:

Dr

Signature:

Anne

Signature numérique de
Anne Roumier-Dauteloup
DN : cn=Anne Roumier-

Date:

09th of July 2018

Please submit a signed and dated copy of this license by one of the following three methods:

1. Upload an electronic version on the JoVE submission site
2. Fax the document to +1.866.381.2236
3. Mail the document to JoVE / Attn: JoVE Editorial / 1 Alewife Center #200 / Cambridge, MA 02140

Rebuttal document for “2-photon imaging of microglial processes attraction toward ATP and serotonin in acute brain slices of young and adult mice” by Etienne et al.

Editorial comments:

Changes to be made by the Author(s) regarding the written manuscript:

1. Please take this opportunity to thoroughly proofread the manuscript to ensure that there are no spelling or grammar issues.
2. Figure 7: Please include a space between numbers and their corresponding units (e.g., 500 μm , 5 μm , etc.). Should “Mean + SEM” be “Mean \pm SEM”? [DONE](#)
3. Movies S1-S3: Please define scale bars in the movie legend. [DONE](#)
4. Table 1: Please provide units for the numbers in the table. [Table 1 has been removed](#)
5. Please revise the title to be more concise if possible. [DONE](#)
6. Please provide an email address for each author. [DONE on the first page of the manuscript.](#)
7. Please shorten the Short Abstract to 10-50 words. [DONE \(42 words\)](#)
8. Please use SI abbreviations for all units: L, mL, μL , h, min, s, etc. [DONE](#)
9. Please include a space between all numbers and their corresponding units: 15 mL, 37 $^{\circ}\text{C}$, 60 s; etc. [DONE](#)
10. JoVE cannot publish manuscripts containing commercial language. This includes trademark symbols ($^{\text{TM}}$), registered symbols ($^{\text{R}}$), and company names before an instrument or reagent. Please remove all commercial language from your manuscript and use generic terms instead. All commercial products should be sufficiently referenced in the Table of Materials and Reagents. For example: Pyrex, Chameleon Ultra2, etc. [DONE](#)
11. Please revise the protocol text to avoid the use of any personal pronouns (e.g., “we”, “you”, “our” etc.). [DONE](#)
12. Please revise the protocol to contain only action items that direct the reader to do something (e.g., “Do this,” “Ensure that,” etc.). The actions should be described in the imperative tense in complete sentences wherever possible. Avoid usage of phrases such as “could be,” “should be,” and “would be” throughout the Protocol. Any text that cannot be written in the imperative tense may be added as a “Note.” Please include all safety procedures and use of hoods, etc. However, notes should be used sparingly and actions should be described in the imperative tense wherever possible. [DONE](#)
13. In the JoVE Protocol format, “Notes” should be concise and used sparingly. They should only be used to provide extraneous details, optional steps, or recommendations that are not critical to a step. Any text that provides details about how to perform a particular step should either be included in the step itself or added as a sub-step. Please consider moving some of the notes about the protocol to the discussion section. [DONE](#)
14. The Protocol should contain only action items that direct the reader to do something. Please move material information (e.g., 3.1.1, 3.2.1, etc.) to the Table of Materials. [DONE](#)
15. 3.2.2: Please specify the age, gender and strain of mouse used. [DONE \(in the Material List\)](#)
16. Step 5: Software steps must be more explicitly explained ('click', 'select', etc.). Please add more specific details (e.g. button clicks for software actions, numerical values for settings, etc.) to your protocol steps. [DONE](#)
17. Please include single-line spaces between all paragraphs, headings, steps, etc. [DONE \(space 12 pts after each paragraph\)](#)
18. After you have made all the recommended changes to your protocol (listed above), please highlight 2.75 pages or less of the Protocol (including headings and spacing) that identifies the essential steps of the protocol for the video, i.e., the steps that should be visualized to tell the most cohesive story of the Protocol.
19. Please highlight complete sentences (not parts of sentences). Please ensure that the highlighted part

of the step includes at least one action that is written in imperative tense. Please do not highlight any steps describing anesthetization and euthanasia.

20. Please include all relevant details that are required to perform the step in the highlighting. For example: If step 2.5 is highlighted for filming and the details of how to perform the step are given in steps 2.5.1 and 2.5.2, then the sub-steps where the details are provided must be highlighted.

21. Discussion: As we are a methods journal, please also discuss critical steps within the protocol and any limitations of the technique. **DONE**

22. Reference 26 is not quoted in the manuscript but in the reference list. Please check. **DONE**

Reviewer #1:

Manuscript Summary:

In their manuscript Etienne et al. describe a protocol for the analysis of microglial processes attraction towards a source of ATP or serotonin gradient using acute brain slices. They also give some important clues to keeping acute brain from slices in optimal conditions, providing the files for the 3D printing of suggested incubation chambers. This is a relevant protocol and I recommend its publication after minor revision.

Major Concerns: None

Minor Concerns:

Please, indicate whether it could be necessary to adapt the proposed 3D printed chamber when using a different microscope.

The recording chamber dimensions are those of a “standard” bathchamber insert, i.e. 62 mm outer diameter. We added these sentences in the Results, 1st paragraph: **“Our recording chamber dimensions are set to fit standard microscopes as they are similar to classical bathchamber inserts (62 mm outer diameter) but as their models are downloadable from supplemental material, the design can be adapted to fit in slice holders of other dimensions.”**

Why should the bit depth of the images be 12 bits or more?

We added a note in the protocol (in 4.1.3) to better explain this: **“NOTE: Higher-bit images allow to distinguish smaller differences in fluorescence intensity than lower-bit images: a change of one gray value in a 8-bit image would correspond to a change of 16 gray values in a 12-bit and of 256 gray values in a 16-bit image. Therefore, higher-bit images are more appropriate for quantitative analysis, but as their size increases with bit depth, storage capacity and computing power can become limiting.”**

Authors indicate that "The frequency of acquisitions is 1 image every 2 minutes". Please, discuss how the frequency of acquisition may affect the temporal resolution of the analysis and the accuracy of obtained data.

The choice of the acquisition frequency is a compromise between the accuracy of the kinetics, the size of the files, and the risk of photobleaching and phototoxicity. We observed that this moderate frequency of acquisition of 1 image every 2 minutes was sufficient to quantify the attraction of processes toward the source of attractant. This frequency has already been used by other groups to measure attraction of microglial processes (e.g. Davalos et al, 2005: 1 image every 2 min; Haynes et al, 2006: 1 image every 5 min) or microglial surveillance - also called “motility” - (e.g. Wu et al, 2008 and Paris et al, 2017: 1 image every 2 min).

However, imaging to measure surveillance is most often performed at 1 image per min (e.g. Madry et al, 2018; Wu et al, 2007; Gyoneva et al, 2013), or faster (e.g. Fontainhas et al, 2011 and Pagani et al, 2015: 1 image every 10 sec).

Indeed, whereas increasing the rate of image acquisition is not critical to measure attraction, which is a net increase of fluorescence over time, it is relevant to improve the accuracy of motility quantification, which is a measure of the turn-over of microglial processes. We thus added a sentence at the end of the discussion : **“However, to quantify the fast extension and retraction rates of microglial processes, and detect potential variations, it would be relevant to increase the acquisition frequency. For example, Pagani et al. use a frequency of one image every 10 seconds²⁸.”**

Authors also suggest reducing the number of Z planes to decrease scanning time, please discuss how reducing the number of Z-planes may affect the resolution/quality of the analysis. In addition, it is indicated to "Select the scan mode XYZT with a Z-interval range at 2 microns". Why could this be relevant? Is this Z-step enough to assure an appropriate 3D resolution? In the same way, is it necessary to use a XY resolution of 1024x1024 (295,07 x 295,07 microns)? Please, briefly discuss this.

A Z-interval range of 2 microns is used in numerous studies performed in 2D (Madry et al, 2018; Davalos et al, 2005; Wu et al, 2007), although a smaller z-interval has been used in recent studies in 3D (1 μm in Paris et al, 2017; 0,4 μm in Heindl et al, 2018). However, Paris et al show in their article that acquisitions with 1 or 2 μm z-intervals give similar quantification of processes and tips velocity. Therefore, the 2 μm z-step interval is appropriate for 3D resolution, at least with the ProMolJ tool (Paris et al 2017). A 3 μm z-interval can also be used to measure attraction (as in Eyo et al, 2014), but this impacts some 3D analysis (Paris et al, 2017), therefore this setting should be the same for all the acquisitions to be compared. Regarding the 1024x1024 XY resolution, it allows a more detailed observation of the processes, which can be relevant for some analysis, but it can be decreased if necessary.

In order to clarify these points in the manuscript, **we changed some explanations in the Note in 4.1.3 in the Protocol.**

Moreover, at the end of the discussion, we added: **“Finally, recent publications described methods to quantify morphological changes or individual processes motility in three dimensions. For such analysis, although a z-step interval of 2 μm is enough for some programs (ref 27), other require a better axial resolution (i.e. z-step 0.4 μm in ref 33.)”.**

Indicate how to exclude z-planes when necessary (first 30 microns).

This has been better explained in the protocol (5.1.2)

Please, indicate the type of Z-stack projection you used (mean, maximum, sum, etc.).

We apologize for this oversight, it is a “Max Intensity Projection”. This is now specified in the protocol (5.1.3).

Indicate whether, when comparing slices, it could be important to analyze 2D images containing information from a similar number of z-slices (similar z-stack thickness). Considering this, in Figure 7A, did the analyzed images of each slice contained information of the same z-thickness?

We perform the z-projection using all the z-slices where fluorescence is visible. This “useful” z-stack thickness may vary but as all the fluorescence is taken into account, we observed no link between this z-stack thickness and the quantification. In addition, the deep z-slices exhibit low fluorescence and contribute scarcely to the signal in the z-projection (that’s why they could be excluded at the imaging step, as indicated in the second Note of 4.1.3 and our answer above).

We now mention this point in the Representative Results, and compare with our methods of quantification and Z-projection: **“To note is that in our protocol the thickness used for the max z-projection encompasses all the z-slices where fluorescence is visible (usually 180-220 μm , see Error! Reference source not found.). Therefore, variations in the absolute number of z-slices does not impact on the quantification of the response. In contrast, some studies use thinner z-stacks (40-60 μm) for z-projection (Ref 6,7,11,27). This is another option, with the risk to exclude some z-slices which exhibit a response as we observed that the attractant effect was visible as far as 70 μm (in z) away from the pipette tip in some experiments. If the thinner option is preferred, it is thus critical to center the z-stack on the pipette tip in z and, importantly, only z-projections done in the same manner (i.e., using all fluorescent z-slices or using a thin z-stack) can be compared.”**

In Figure 7A, the z-thickness in the initial figure were from 180 to 280 μm but considering the point raised by the reviewer, in order to standardize the protocol and make it clearer, we updated the Figure 7A using values obtained from 180-200 μm z-thickness projections (i.e. excluding eventually the deepest z-slices, which had indeed very little fluorescence).

In figures, please, indicate the z-thickness of the images shown.

They are now indicated in the figure legends.

Please, discuss the possibility of analyzing images in 3D, without using Z stack projections, maybe using a sphere (circular ROIs of decreasing radius from the central plane where the tip of the pipette is detected) as a 3D ROI for quantification.

The advantage of a morphological analysis in 2D as the one proposed in this manuscript, *versus* in 3D, on z-stacks, is that it requires less computer power and can be performed straightforward using simple image analysis tools. A limitation is that, by definition, the z-projection leads to underestimation of the growth of the microglial processes, by masking the movements in the z dimension. The suggestion of using circular ROIs with decreasing radius (taken into account the distance between two consecutive z-plans) is very interesting and should logically lead to a slightly higher, and more accurate, estimation of the fluorescence increase near the pipette tip. Nevertheless, this would require a specific macro, in order to apply different ROI on the different z planes, and a very precise localization of the pipette tip in the 3 dimensions. Therefore, we believe that this goes beyond the aim of this manuscript, which is to provide a simple technique for researchers who would like to start investigating the morphological dynamics of microglia, even though they are not familiar with image analysis. For researchers who would like to pursue on this, we provide references on 3D analysis tools in the Discussion part.

Mean intensity may be affected by changes in the expression of the fluorescent protein after treatment, thus a process already included in the initial ROI may increase the intensity of its fluorescence. Please, indicate how this could affect the interpretation of the data and suggest at least an alternative approach to correct or overcome this problem.

We agree with this remark, in theory, but in the experiments we describe, the increase of fluorescence is visible in the first minutes after injection. Because of this rapid effect, increased expression of the gene encoding the fluorescent protein could not contribute to the increase in fluorescence. This could be an issue for long-term imaging, but it is unlikely when imaging lasts no more than 30 minutes after treatment.

An alternative approach to overcome this problem is to draw manually and measure at each time point the area not covered by microglial processes. This method was mentioned in a note of the protocol, but taking into account the remark of the reviewer, we have rephrased the sentence to briefly presented the advantage and disadvantage of this method, and moved it to the Discussion part: **“an alternative method which does not depend on the fluorescence level of the microglial processes, but requires more actions of the experimenter for the image analysis, is to measure the reduction of the empty space around the pipette tip after compound application ref 11,32.”**

Reference 26 is not mentioned in the manuscript.

This has been solved (formatting problem).

Please, discuss the quantification method and compare your data with those from other studies.

Our quantification method is inspired by the method used by Davalos et al 2005.

As suggested, we compared, in the Representative Results, our data with those from other studies using the same kind of quantification method: **“The effect of ATP is in the same range than those obtained by other groups with a similar method in vivo (Davalos et al, 2005: 0.53; Haynes et al, 2006: 0.413)**

and in slices (Dissing-Olesen et al, 2014: 0.8 ref5 if normalized as here; Pagani et al, 2015: 0.6 ref28). Differences can come on one hand from biological parameters: the slice preparation method, the amount of ATP injected, the age or the brain region, and on the other hand from analysis parameters: the diameter of the ROI and the thickness of the z-stacks used for the z-projection (i.e., the whole thickness where fluorescence is detected, or only the 40-60 µm around the pipette tip, where the maximal response is expected).."

Reviewer #2:

In this study, Etienne et al. characterized a detailed protocol to study microglial processes chemotaxis towards ATP or serotonin in acute brain slices. Microglial dynamics are useful information to understand microglial function in health and disease. The protocol is very well described and would be valuable for the microglial research. Here are some minor concerns need to be addressed:

1. When introducing ATP-induce microglial process chemotaxis, the authors omitted the earliest characterization of this phenomena using ATP-pipette in acute brain slices (Wu et al., *Glia*, 2007). In addition, the paper is the first to combine microglia electrophysiology and time-lapse live imaging to study mechanisms underlying ATP-induced microglia process chemotaxis.

We apologize for this oversight and this princeps study is now cited in the introduction.

2. Also, it is not correct to state that microglia process attract to glutamate (in abstract and introduction). Many studies have shown that glutamate cannot directly induce process chemotaxis, but most indirectly caused by glutamate-triggered ATP release (Wu and Zhuo, *J Neurophysiol*, 2008; Eyo et al., *J Neurosci*, 2014; Dissing-Olesen et al., *J Neurosci*, 2014; Wendt et al., *J Neurosci*, 2016).

For sure we know that the effect of glutamate is not direct, and we regret that the sentences were confusing.

In the abstract, we don't mention glutamate anymore (indeed, by shortening the sentence, we had ended with a wrong statement). In the introduction, we have added this sentence (1.67): **"These effects either are directly mediated by microglial receptors (for ATP and norepinephrine) or require ATP release from neurons (for NMDA)."** as well as the reference to Eyo et al., *J Neurosci*. 2014 in addition to Dissing-Olesen et al, 2014.

3. Line 93, page 3. The authors cited Gan's paper about imaging microglia using YFP. This is actually a wrong statement, because the mice do not have strong fluorescent signals for live imaging.

It is true that the fluorescent signal in these mice is much lower than in the CX3CR1^{GFP/+} mice, and that microglia imaging in their brain slices is challenging. However, with some changes in the acquisition parameters, we were able to record microglia processes attraction toward ATP and 5-HT and to perform the analysis described in the protocol. A movie performed on these mice is provided for the reviewer (not

to be included in the manuscript). As these mice are available and are useful tools to combine genetic deletion and imaging, we think they deserve to be mentioned, but we changed the text of the Note in 4.1.3 to strengthen the fact that it is more difficult than with the CX3CR1^{GFP/+} line and requires optimization of the acquisition parameters : **“NOTE: It is possible to perform similar experiments on slices from CX3CR1creER-YFP mice, a mouse line used to induce genetic deletion in microglia only, and which microglia constitutively express YFP. However, the expression level of YFP is very low compared to GFP in CX3CR1GFP/+ mice, thus imaging is possible but challenging and require optimization of the acquisition parameters. We propose to adjust them as follows:...”** .

4. For ATP delivery, no microinjection is needed to induce microglial process chemotaxis. As soon as ATP-containing pipette is inserted into the brain slices, it forms the ATP gradient that can induce process chemotaxis towards the pipette. This should be discussed.

We sometimes observed such effect, but it was moderate in comparison with the effect of injection. To note is that we use an ATP concentration of 500 $\mu\text{mol.L}^{-1}$, which is less than in many studies (e.g. Wu et al, 2007 and Eyo et al, 2014: 3 mmol.L⁻¹; Dissing-Olesen et al, 2014 : 4 mmol.L⁻¹; Haynes et al, 2006 : 20 mmol.L⁻¹), and may explain our moderate attraction in absence of injection.

Nevertheless, this issue is now discussed in the Protocol, 4.2.6: **“NOTE: leakage of ATP out of the pipette can attract microglial processes even before injection (if this occurs, it will be visible at the analysis step). Although this should be moderate with the ATP concentration used (500 $\mu\text{mol.L}^{-1}$), if it is an issue, consider prefilling the micropipette with 2 microliters of ACSF prior to add the ATP (or other compound) solution at 4.2.6.”**.

5. The analysis of microglial chemotaxis is a bit simple. The authors should discuss recent studies using 3D analysis of microglial process dynamics (Paris et al., Glia, 2018; Heindl et al, Front Cell Neurosci, 2018). Also, why 35 μm diameter was used for analysis?

We agree that the quantification is simple, but the aim of our manuscript is to provide experimenters genuine to the field with an easy-to-implement procedure. Actually, in the lab we initially used a more complex quantification of the processes growth (see in Kolodziejczak et al 2015), but finally moved to the method presented here, which is more straightforward. The studies mentioned for 3D analysis have been developed to quantify microglial surveillance (Paris et al, 2018), and the complexity of microglial ramification (Heindl et al, 2018), but not specifically the chemoattractant effect. We nevertheless agree that 3D analysis provide more detailed data and these two studies are now presented in the Discussion (l. 743-746).

Regarding the diameter of the ROI used for analysis, it is the same than the one used in Davalos et al, 2005. Smaller (20 μm diameter in Pagani et al, 2015) or larger diameters (70 μm diameter in Haynes et al, 2006; 100 μm diameter in Dissing-Olesen et al, 2014) are also found in the literature. In order to address quantitatively this question of the reviewer, we reanalyzed a series of experiments with ROI of different sizes and the results are now discussed in Figure 7B (l. 551): **“Figure 7B shows how the size**

of the ROI also impacts on the quantification, here of ATP-induced processes growth. Increasing the diameter from 35 (the diameter used in Figure 7A and for all our analysis) to 50 or 70 μm reduces variability among experiments (slices) by suppressing the issue of the small R1 positioning. However, it also decreases accuracy and the magnitude of the detected response. Indeed, with larger ROIs, there is more background due to processes or cell bodies not affected by the treatment, and a growth of processes can be partially blunted by the concomitant retraction of microglial branches more distant from the pipette but nevertheless inside the ROI. In conclusion, it can be relevant to use ROIs different than a 35 μm diameter circle, but it is fundamental that the ROI is always the same in all the data-sets to be compared.”

Reviewer #3:

2-photon imaging of microglial processes attraction toward ATP or serotonin in acute brain slices of young and adult mice.

The manuscript by Etienne et al. focuses on the imaging and analysis of microglial motility towards a source of ATP or 5HT in acute brain slices. The topic is of high interest and the methods described will be useful to researchers in the microglial field. The method is well explained and touches upon different ways to improve slice health. The manuscript, however, could be improved by addressing the following comments.

The authors describe the injury induced-like movement of microglia towards an ATP or serotonin source, but do not address why an experimenter would use one chemotactic source versus the other. A slightly more detailed introduction covering the benefits of imaging this type of motility and what sort of biological questions that could be answered would help the reader decide on the exact methodology to use.

We have modified the introduction following these recommendations. Notably, the different forms of morphological plasticity are presented in the introduction.

The interface slice chamber and the dual perfusion imaging chamber the authors describe are quite interesting. They claim that using these significantly improves slice health and extends their use compared to using other standard aCSFs, maintaining the slices submerged prior to imaging and imaging in a bath with the slice touching the coverslip. Could they provide an estimate of by how much the health of the slice is improved and which of the modifications they believe to be the most important?

Unfortunately, it is difficult to tell quantitatively by how much the health is improved because our final protocol results from several modifications that were tested and added over time, and which finally allowed us to achieve more robustness and a better reproducibility in our experiments than at the beginning. Several modifications probably contribute synergistically to the global improvement, and it would be difficult to establish a hierarchy among them. Nevertheless, in the Discussion, we highlighted

the mechanisms by which the specificities of the protocol may improve the viability and indicated references of previous studies addressing them separately (1.696-729).

With respect to making the chambers, it is unclear how the different parts come together- are they glued together? More information on building the chambers would be helpful.

They don't need to be glued because they fit perfectly together. This is now explained in the Protocol (3.1.3.2, 4.2.1) and in the Results (1.442-444).

The slices are maintained in an interface chamber until ready for recording- more details on the amount of liquid above the nylon mesh and how the slices are prevented from drying should be provided.

This is now detailed in the Protocol (3.1.3).

The authors state the infrared laser is tuned to 920nm and used with 5-15% power- what does this translate to in terms of actual power at the objective (in mW/cm²)?

This information has been added (4.1.2): **“This corresponds to a power of 3 - 5 mW under the objective”**.

The image analysis is done in 2D, which I understand is a common limitation in this field of research. However, more information should be provided on things that should be taken into consideration when comparing different datasets- eg. the size of the z stack, the positioning of the pipette tip, the size of the ROI, etc.

Image analysis in 2D is a limitation if the aim is to quantify the motility of individual processes - or, more exactly, it does not allow to measure the real distance traveled by the tips of microglia, but we believe is not the case when quantifying a global attraction toward a local source of a compound, as we do here.

If 3D analysis has to be performed, the z-interval can have an impact, depending of the analysis plugin. If the aim is to measure the speed of the changes affecting the processes, either in 2D or 3D, the sampling rate has a strong impact. We added informations on these two points in the Discussion:

(1.740): **“to quantify the fast extension and retraction rates of microglial processes, and detect potential variations, it would be relevant to increase the acquisition frequency. For example, Pagani et al. use a frequency of one image every 10 seconds”**.

(1. 743): **“Finally, recent publications described methods to quantify morphological changes or individual processes motility in three dimensions. For such analysis, although a z-step interval of 2 μ m is enough for some programs²⁷, other require a better axial resolution (i.e. z-step 0.4 μ m in 33)”**.

In addition, we thank the reviewer for raising the point of things to be taken into consideration to compare datasets. We now discuss the different parameters along the Representative Results and Discussion, and have notably added a Figure (7B) to compare the impact of the ROI size. We hope these comments will be helpful to design and compare experiments.

Similarly, no information is given on how to deal with photobleaching over time. If photobleaching occurs then it is possible that the mean intensity ROI plot will give a flatline despite clear processes moving towards the source.

We agree with the reviewer that photobleaching is an important issue which may lead to underestimation of the processes attraction. For our experiments, we checked that our excitation and acquisition parameters did not induce any photobleaching and it is confirmed by the stable fluorescence over time of the slices treated with ACSF (Figure 7C). However, as photobleaching could create a serious bias, in the new version of the Results we gave more information about photobleaching, how to check for it and how to limit it (l. 575): **“As it can bias measurements, it is important to rigorously check that there is no photobleaching in the experimental conditions. To do this, we recommend to acquire a XYZT series on a slice with GFP-expressing microglia, for 30 minutes (ACSF can be injected, but actually no stimulation is needed), with the excitation and acquisition parameters set as in the experimental conditions. Then, a quantitative measure of the fluorescence over time in different regions of interest, including microglia cell bodies or processes, will reveal if there is a gradual loss in emission intensity, usually an exponential decay, indicating photobleaching. If it is the case, some adjustments can be performed: re-alignment of the laser, reduction of the laser power and increase of the detector gain, reduction of the number of z-planes and increase of the interval between them to limit illumination. Photobleaching is favored by high power or long (ex: repeated illumination for line averaging) excitation, one must thus pay particular attention to it if a sustained illumination is used to image cells with low fluorescence”**.

In the representative results the authors show high variability in results between slices- the highest response is approximately 3-fold greater than the lowest. A discussion of this and limitations of the methodology when a small effect size is predicted should be included

We now discuss possible sources of variability in the Representative Results. We chose not to address here the question of the number of samples to use depending of the variability and the expected effect size, as this is a concern for statistics in general, not specific for this technique.

In addition, we would have liked to compare the variability in Figure 7A with those in other studies using similar techniques, but it was not possible as the raw results are generally not shown in publications. The SEM however is in the same range than those found in similar studies.

The paper would benefit from a troubleshooting section to cover the above points

To our knowledge, the format of JoVE publication does not include a troubleshooting section. We therefore used Notes in the protocol, or comments in the Results and Discussion parts, to cover these important points and hope that the reader will find the relevant informations

Minor comments

The grammar should be reviewed throughout

We have now reviewed the manuscript to our best.

The second paragraph of the introduction has no references beyond the first sentence

Two references (Stence et al, 2001 and Kurpius et al, 2006) have been added.

Becher I believe is beaker in English

Thank you, we changed this.

Figure 3B the lettering is difficult to see

Lettering size has been increased.

Figure 6 the arrows and arrowheads are difficult to distinguish from the cells. This figure would benefit from being in colour.

They are now bigger and in red.

Are the micropipettes used made from thin or thick walled glass?

They are made from thin wall capillaries. This was said in the material list but has been added in the protocol.

Reviewer #4:

The manuscript provides an experimental protocol for analysing the morphological dynamics of microglial cells in acute brain slices.

Overall, it is fairly well written and organized, providing practical information on how to maintain / improve the quality of the biological sample and the imaging data. While it mostly rehashes previously published information, it does provide useful insights and reminders on how to prepare and maintain live brain tissue sample, which is very sensitive.

Thus, the protocol could be a handy resource for researchers entering the microglia field, as 2-photon microscopes and fluorescently labelled mouse lines have proliferated.

Comments and suggestions to improve the manuscript:

* Stating the % values of laser power is useless; absolute IR power after the objective should be provided. This is important for comparing the threshold for inducing phototoxic effects between different experimental conditions, mice, users, labs etc.

This information has been added (4.1.2): **“This corresponds to a power of 3 - 5 mW under the objective”**.

* There is no point in Table 1, which lists the settings for a particular type of pipette puller, as many labs likely have a different one. Instead, they could show images of the tip of the pipette and its best geometry.

Table 1 has been removed.

* A pixel resolution of 295 nm is a bit low, given the optical resolution of their 2-photon microscope and the thin size of microglial processes. I would recommend at least 200 nm to comply with the sampling theorem and not to throw away information needlessly.

Indeed, having a better xy resolution could be interesting for a detailed reconstruction of microglia morphology as in Heindl et al, 2018, which uses a resolution of 200 nm, and we will consider this suggestion for future experiments. However, for our global analysis of fluorescence, it was not a problem, and indeed we preferred to image larger fields with lower xy resolution in order to see microglia affected and not affected by the injection. In addition, in the literature, when the information is available, similar or lower resolution (i.e. larger pixel dimension) is used to quantify microglia motility (Madry et al, 2018 : 400-450 nm) and even to track processes (Paris et al, 2018 : 497 nm), so we chose not to comment this specific point in the manuscript.

* A temporal resolution of 1 stack of images every 2 minutes seems too low to capture the rapid dynamics of microglial processes.

The choice of the acquisition frequency was a compromise between the accuracy of the kinetics, the size of the files, and the risk of photobleaching and phototoxicity. We observed that this moderate frequency was sufficient to quantify the attraction of processes. This frequency has already been used by other groups to measure attraction of microglial processes (e.g. Davalos et al, 2005: 1 image every 2 min; Haynes et al, 2006: 1 image every 5 min) or microglial surveillance - also called “motility” - (e.g. Wu et al, 2008 and Paris et al, 2017: 1 image every 2 min).

However it is true that whereas increasing the rate of image acquisition is not critical to measure attraction, which is a net increase of fluorescence over time, it is relevant to improve the accuracy of motility quantification, which is a measure of the turn-over of microglial processes. Consistent with that, imaging to measure surveillance is most often performed at 1 image per min (e.g. Madry et al, 2018; Wu et al, 2007; Gyoneva et al, 2013), or faster (e.g. Fontainhas et al, 2011 and Pagani et al, 2015: 1 image every 10 sec). We thus now comment in the Discussion (l. 740): **“to quantify the fast extension and**

retraction rates of microglial processes, and detect potential variations, it would be relevant to increase the acquisition frequency. For example, Pagani et al. use a frequency of one image every 10 seconds”.

* The authors claim that a choline-based ACSF aids the health of the brain slices and microglia. This should be supported by data or literature references.

Two references addressing this point have been added in the Discussion (l.700-701).

* The paper by Pagani et al (Front Cell Neurosci. 2015) should be cited, where similar methodological information was presented in detail.

This study quantify attraction with another method and we agree that it is interesting to both. Pagani et al, 2015 is thus now cited and commented, notably in the Discussion (l.742).

* The first paragraph of the Discussion should be compressed and made more relevant.

We followed this advice and shortened this paragraph.

* Usually, after cutting brain slices are left to recover for at least one hour before the start of any recordings, according to the consensus in the electrophysiology field. So, it is unexpected that they used a much shorter period.

Re-reading the manuscript, we realized that indeed we had not provided proper information on the recovery step, and it resulted confusing, thank you for raising this point.

We have completed the protocol in 3.2.9 to explain that after the first 10 min recovery in cool choline-aCSF, the slices are transferred to and maintained in the interface chamber for a least 30 minutes before imaging. It is still less than the standard time in electrophysiology, but we didn't observed changes in the microglia response to compounds when slices had recovered for 1h, instead of 30 minutes, in the interface chamber. To note is that several groups let the slices recover less than 1 hour for microglia imaging (e.g. : Eyo et al, 2014 : 30 min of recovery ; Madry et al, 2018: 30 minutes of labeling after slicing and before imaging).

However, as we cannot exclude that a longer recovery would be relevant in certain conditions, we mention in the Discussion that (l. 712): **“Afterwards, slices were transferred into the interface holding chamber to recover for an additional minimum time of 30 minutes. The duration of this second recovery period could be optimized according to the brain area of interest, the Na⁺ substitute, and the age of the animal, and it should last at least 1 hour if electrophysiology has to be performed in parallel with imaging”**.

* To obtain more reproducible results, the use of automated pressure devices (e.g. picospritzer) are preferred over manual operation of syringes.

This was mentioned in the protocol, but we have rephrased the Note for better clarity (4.2.12) and commented on this point in the Results (1.548): **“Therefore, to detect small effects or variations, it may be interesting to use an automatic device for the compound injection”**.

* It is stated that the injection pipette is placed just on top of the slice, but it is hard to imagine how a local effect can be induced inside the slice unless the pipette really penetrates into the slice. For this a finer tip (<2 microns) may be necessary.

We apologize if this was unclear, but the tip of the pipette actually penetrates 80-100 μm below the surface of the slice, as shown in Figure 3B. Relevance of this point and parameters that may influence it are now commented in the Results (1.451): **“...its thin extremity entered slightly into the tissue, down to 80-100 μm from the surface. It is important that the pipette is not too superficial because it may not deliver the solution correctly onto the cells, nor enter too deep because it may reach a region where fluorescence signal is too low. Parameters that may affect the depth reached by the pipette tip are the angle of the pipette, which can be adjusted with the 3-axis micromanipulator, and the pipette mouth diameter”**.

* Figure 4: the panels A and B are too redundant, consider merging with finer overlay of the graphics.

We followed this advice.

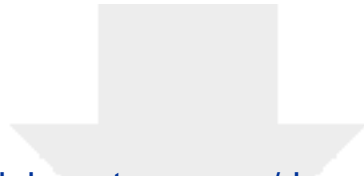
* Figure 5: consider showing more time points and zooming in on ROI to illustrate better the directional motility effect after compound injection.

Insets zoomed on the ROI have been added on each picture. We did not add more time points here to avoid having a too crowded figure, but an intermediate time point for ATP is shown in Figure 4.



Click here to access/download
Supplemental Coding Files
Figure S1_Imaging chamber.stl





[Click here to access/download](#)

Supplemental Coding Files

Figure S2_Interface holding chamber.stl

